



UNITED NATIONS
UNIVERSITY

GEOTHERMAL TRAINING PROGRAMME
Orkustofnun, Grensasvegur 9,
IS-108 Reykjavik, Iceland

Reports 2011
Number 24

BOREHOLE GEOLOGY AND HYDROTHERMAL ALTERATION OF WELL HE-55 AT HELLISHEIDI GEOTHERMAL FIELD, SW-ICELAND

Ngereja Myabi Mgejwa

Ministry of Energy and Minerals
Energy and Petroleum Affairs
P.O. Box 2000
Dar es Salaam
TANZANIA

nmmgejwa@yahoo.com, n.mgejwa@mem.go.tz

ABSTRACT

Well HE-55 is located in the southern part of Hellisheidi geothermal field, west of the Hverahlid geothermal area. The well was drilled as a multi-purpose well aimed to strike NE-SW trending faults and fissures west of the well. This report will focus on data from geological logging of the upper 1000 m depth. A binocular microscope, a petrographic microscope, XRD-analysis, a fluid inclusion analysis and geophysical logs were used to gather data. Small circulation loss was encountered at a depth of 258-274 m with a maximum of 6 l/s and a minimum of 2 l/s. Different rock types were encountered in the well such as fine- to medium-grained basalt, medium- to coarse-grained basalt, basaltic tuff, basaltic breccias, glassy basalt and diamictites. The surface is covered by fine- to medium grained postglacial lava, but the well is dominated by hyaloclastite formations, and interglacial lavas which are intruded by some dykes of basaltic composition. The upper 1000 m have four hydrothermal alteration zones ranging from low-temperature alteration to high-temperature: unaltered zone (< 50°C); smectite-zeolite zone (50-200°C); chlorite-epidote zone (250-275°C); and epidote-actinolite zone (275-350°C). Each zone is indicated by the appearance of index minerals that represent each zone. Calcite appears to be the dominant alteration mineral in the well and tends to deposit later than higher temperature alteration minerals which may suggest cooling of the system, supported by the observation of higher alteration temperatures than formation temperatures. Most of the homogenization temperatures of fluid inclusions from three different depths showed cooling of the system with time. Seven small aquifers were identified at 258, 274, 362, 450, 660, 765 and 988 m. Stratigraphic correlation between wells HE-55, HE-36 and HE-57, which are relatively close to one another, is practically impossible except for the upper parts of HE-55 and HE-57, where identical patterns of an interglacial lava sequence were found. In addition, a pillow basalt formation in the upper parts of HE-36 and HE-55 could probably be correlated as the descriptions of the formations were similar in petrographic analysis.

1. INTRODUCTION

1.1 General information

The Hellisheidi high-temperature geothermal field is located in SW-Iceland; it forms a part of the Hengill geothermal system and is situated in the southern sector of the 110 km² Hengill low-resistivity anomaly. The Hengill central volcano lies at a triple junction where the western rift zone, the Reykjanes Peninsula and the South Iceland Fracture zone meet. The Hellisheidi high-temperature field has four potential geothermal fields: Skardsmýrarfjall, Hverahlíd, Gráuhnúkar and Reykjafell. Well HE-55 is located within the Hverahlíd field in the southeast sector of the Hengill area.

Well HE-55 is one of 57 production wells which have been drilled since 1985 in the Hengill area for the purposes of power generation and production of hot water for space heating in the industrial and domestic sectors of the Reykjavik area; the provider is Reykjavik Energy. Around 2/3 of the primary energy in Iceland comes from geothermal energy, while for Tanzania about 90% of the primary energy is biomass based energy.

HE-55 was drilled to 2782 m measured depth and cuttings were sampled at 2 m intervals for analysis, identification of subsurface formations, the location of aquifers or feed zones and the determination of the alteration temperatures. Binocular analysis of well cuttings, petrographic analysis of thin sections, X-ray diffractometer tests, a fluid inclusion analysis and interpretation of geophysical logs are the analytical methods used in this study to explore the upper 1000 m of the well.

This study is part of a six month training course at the United Nations University Geothermal Training Programme (UNU-GTP) in Iceland in 2011. The objective was to obtain practical experience in geothermal energy, especially in borehole geology, and also to assess the geothermal system history and lithology of well HE-55 at Hverahlíd - Hellisheidi geothermal field.

1.2 Regional geology

Geologically, Iceland is very young compared to Tanzania which has Archean, Proterozoic rocks and young rocks. The oldest rocks in Iceland are about 16 m.y. and the island is still growing (Hardarson et al., 1997). It is located in the North Atlantic Ocean, south of the Arctic Circle, and lies across the Mid-Atlantic Ridge between the Eurasian and North-American plates (Figure 1). The two plates are drifting apart approximately 1 cm per year in either direction (Figure 1) so, mathematically, in one million years the separation will be approximately 20 km. Iceland is located above a mantle plume which is the source of this biggest landmass on the Mid-Atlantic Ridge. Currently, the plume stem reaches the lithosphere under Vatnajökull glacier (Figure 2), about 200 km southeast of the plate boundary defined by the Reykjanes- and Kolbeinsey Ridges

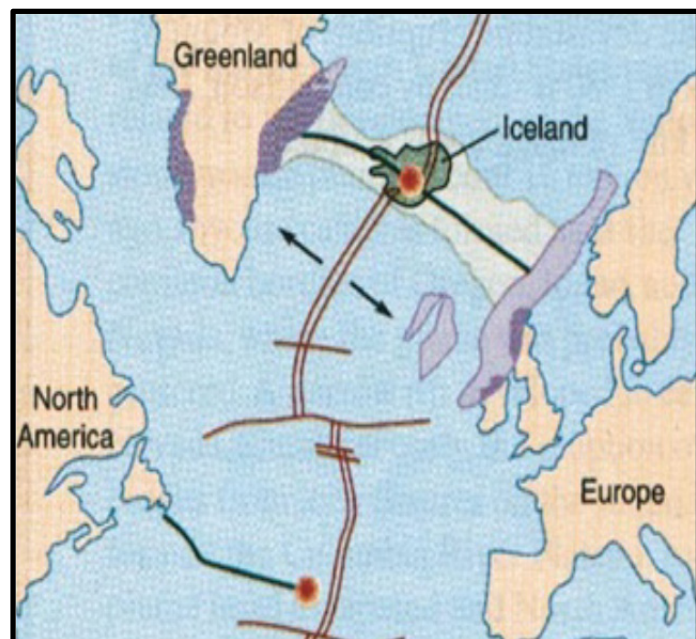


FIGURE 1: Location of Iceland; the orange circle indicates the location of the Icelandic plume and the arrows show the spreading direction (taken from Njue, 2010); the heavy black line, across Iceland, shows the location of the Greenland- Iceland-Faeroes Ridge

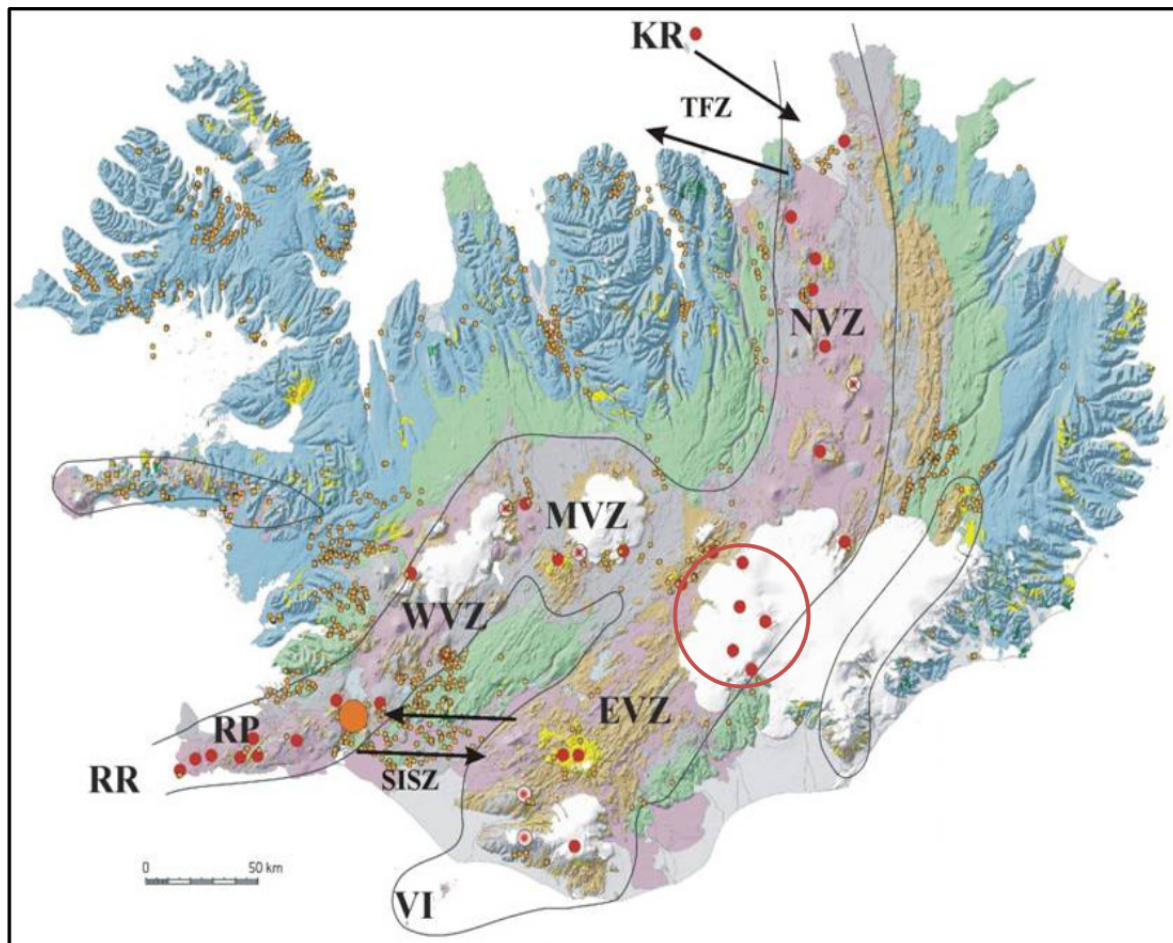


FIGURE 2: Geological map of Iceland showing location of the active volcanic zones and transform faults. RP=Reykjanes Peninsula; WVZ=Western Volcanic zone; MVZ=Mid-Iceland Volcanic Zone; NVZ=Northern Volcanic Zone; EVZ=Eastern Volcanic zone; VI=Vestmanneyjar Islands. SISZ=South Iceland Seismic Zone; TFZ=Tjörnes Fracture Zone; Orange filled circle represents the approximate location of the Hengill volcanic system. Red dots indicate high-temperature geothermal fields and red circle shows the approximate location of the Icelandic plume centre (adapted from Jóhannesson and Saemundsson, 1999)

(Wolfe et al., 1997). The formation of Iceland is due to the eruption of volcanic materials from underneath due to rifting and crustal accretion along the NE-SW axial rift system.

With the mantle plume and the Mid-Atlantic Ridge crossing Iceland, crustal spreading results in older rocks being found to the east and the west of the island while the youngest rocks are found in the central rift zone. As a result of its unique location, Iceland is one of the most active and productive subaerial regions on Earth, with an eruption frequency of more than 20 events per century and a magma output rate of about 8 km^3 per century in historic times, i.e. over the last 1100 years (Thórdarson and Höskuldsson, 2008). The surface geology is entirely composed of igneous rocks of which about 80-85% are basaltic in composition; acidic and intermediate rocks compose about 10%. The amount of sediments of volcanic origin is 5-10% in a typical Tertiary lava pile, but may locally be higher in Quaternary rocks (Saemundsson, 1979).

Volcanic rocks in Iceland are classified into three series: tholeiitic, alkali and transitional alkali. The tholeiitic rock series is confined to volcanic systems in the rift zones which delineate the crest of the Mid-Atlantic Ridge. The alkali and transitional series are confined to volcanic systems in the flank zones (Jakobsson et al., 2008).

1.3 Tectonic setting

Iceland is the only subaerial part of the Mid-Atlantic Ridge and, while the North Atlantic is spreading symmetrically away from the mid-ocean ridge (Hjartarson, 2009), the ridge system as a whole migrates over the plume to the northwest resulting in repeated shifts of the spreading axis through rift jumping to the southeast (Saemundsson, 1979; Hardarson et al., 1997). The shift of the plate boundary can therefore be explained as a response to the gradual northwestward drift of the plate boundary away from the central plume upwelling under Iceland (Hardarson et al., 1997). Being at the intersection of two major structures, namely the Mid-Atlantic Ridge and the Greenland – Iceland – Faeroes Ridge (Figure 1), the island is home to approximately 60% of the world's fissure eruptions.

The Mid-Atlantic Ridge is a constructive plate boundary while the Greenland-Iceland-Faeroes Ridge is thought to be the trail of the Icelandic mantle plume, active from the time of the opening of the North Atlantic Ocean 60 million years ago to the present (Sigmundsson and Saemundsson, 2008). The centre of the mantle plume is located below Central East Iceland (Figures 1 and 2) below the volcanic rift zone which crosses Iceland from southwest to northeast and is divided into two parallel branches in South Iceland (Pálmason and Saemundsson, 1974).

In South and North Iceland, the Mid-Atlantic Ridge has been displaced to the east by transform faults (Figure 2) which are defined as fracture zones. The southern fracture zone is called the South Iceland Seismic Zone (SISZ) while the northern one is called the Tjörnes Fracture Zone TFZ, shown in Figure 2. The volcanic rift zone is, thus, a zone of active rifting and volcanism and is characterised by well-developed extensional structures such as tension fractures, normal faults and grabens with dykes and normal faults occurring at deeper levels (Gudmundsson, 1998). Dauteuil et al. (2005) explained that the active zone has at least doubled in width over the last 200,000 years, and forms a unique wide area ranging from 200 km in the south to 120 km in the north. Gudmundsson (1992) stated that the swarms may be up to 5-10 km wide and 40-80 km long and make up most of the volcanic rift zone. The volcanic rift zone is about one-third of the area of Iceland.

1.4 Hengill Volcano

The Hengill central volcano is located approximately 30 km from the capital city of Reykjavik and is a component of a 40-60 km long fissure/fault swarm, part of the western volcanic zone (Figure 2). The greater Hengill volcanic complex is related to three distinct volcanic systems. The oldest system is the eroded Pleistocene Hveragerdi – Grendalur (Graendalur) volcanic system (Figure 3). Then there is Hrómundartindur, the smallest of the three systems, in which the latest recorded

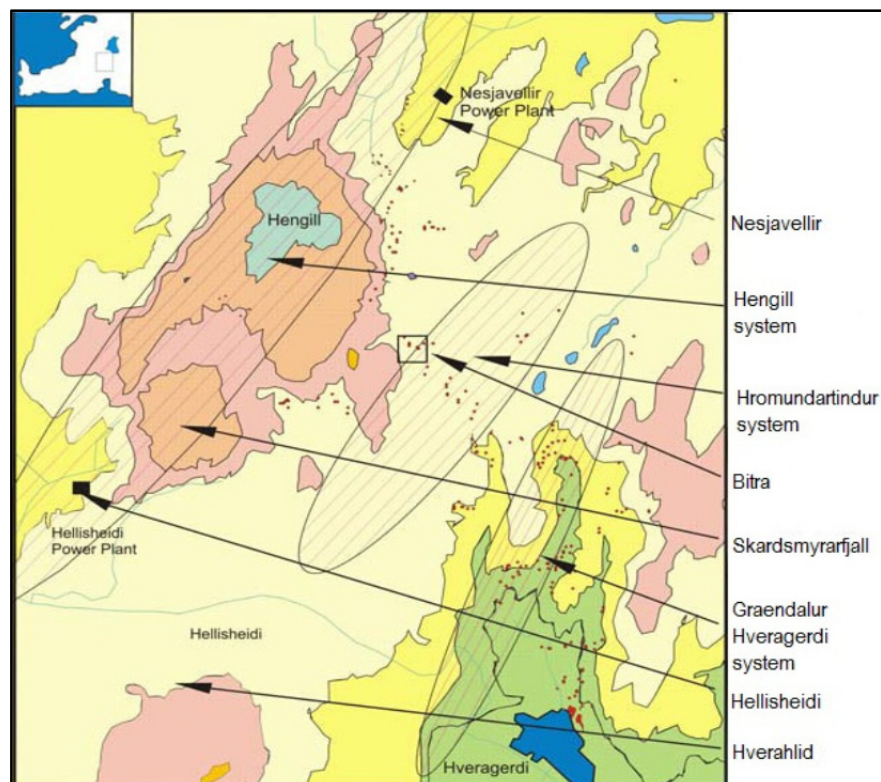


FIGURE 3: The greater Hengill volcanic complex (from Pendon, 2006)

eruption dates back to 10,000 years ago (Foulger and Toomey, 1989). These systems are extinct in terms of volcanic activity but are still active seismically and host geothermal reservoirs (Foulger and Toomey, 1989).

Hengill is the youngest and most active of the three volcanic and geothermal complexes. There are four geothermal fields in Hengill, one of which is Hellisheidi, located southwest of the volcano, in which the Hverahlid field is found (Figures 3, 4 and 5).

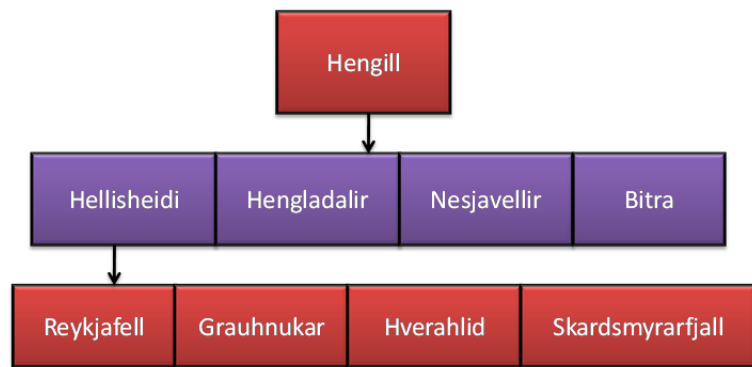


FIGURE 4: Classification of the Hengill geothermal fields

The main NE-SW fractures of the Hengill system are intersected by easterly striking features that possibly affect the permeability of the Hellisheidi field (Árnason, 2007; Hardarson et al., 2010). Volcanic fissures of 10.3, 5.5 and 2 thousand years (Figure 5) seem to play an important role as major outflow zones in the field (Saemundsson, 1995; Björnsson, 2004; Franzson et al., 2005; Franzson et al., 2010). The geothermal activity of the Hengill central volcano and its fissure swarms is explained by one or more up-flow zones underneath the Hengill volcano (Franzson et al., 2010). The up-flow is caused by buoyancy as hot intrusions in the roots of the volcano heat up groundwater. This, on the other hand, also creates a pressure-low deep under the volcano so fluids from the outer boundaries of the system recharge the up-flow (Franzson et al., 2010). These fissures have been one of the two main drilling targets in the Hellisheidi field. Large NE-SW fault structures at the western boundary of the Hengill graben, with more than 250 m total throw, have also been targeted. In addition they have also been used as targets for reinjection wells in the area (Franzson et al., 2010; Hardarson et al., 2010).

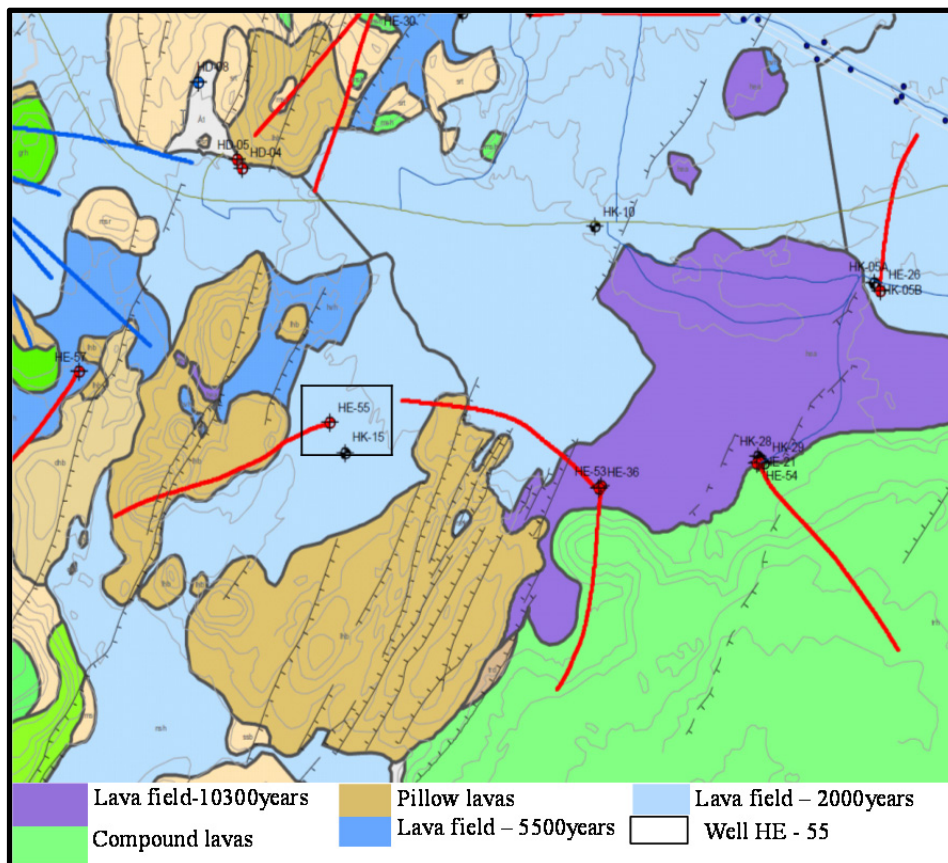


FIGURE 5: Geological map of the Hverahlid geothermal field (mod. from Saemundsson, 1995)

1.5 Previous studies at the Hverahlíd area

The Hverahlíd surface area is characterized by two main features: hyaloclastite formations which were formed subglacially, and postglacial volcanic fissure swarms trending NE-SW. The age of the older is 5500 years and the younger is about 2000 years (Saemundsson, 1995).

The subsurface lithology in the Hverahlíd high-temperature field is mainly composed of two rock types: hyaloclastites and interglacial lava series. The lava series are common formations and were formed during postglacial and interglacial periods (Helgadóttir et al., 2010; Nielsson and Franzson, 2010). This makes Hverahlíd somewhat different from the rest of the Hengill system, which is dominated by hyaloclastites. Nielsson and Franzson (2010) pointed out that the reason for this difference may be that the Hverahlíd field was outside the area of main volcanism of the central volcano during the glacial periods.

There are two types of intrusive rocks in the Hverahlíd high-temperature system (Nielsson and Franzson, 2010), dominant fine-grained basalt intrusions and minor intrusives of andesitic to rhyolitic compositions. The fine-grained nature of the intrusions indicates that they are dykes and/or sills. The intrusions are rare down to about 800 m b.s.l. but become more numerous at deeper levels. Below 1600 m b.s.l. the intrusive rocks become the dominant part of the lithological succession (Nielsson and Franzson, 2010).

Geophysical studies carried out in the Hengill area, including the Hverahlíd area, show a low-resistivity layer in the uppermost part which may indicate a smectite-zeolite alteration zone; high resistivity in the deeper part may indicate the high-temperature core of the system. Figure 6 shows the low resistivity associated with the Hengill area at 400 m below sea level, and HE-55 is found within that area.

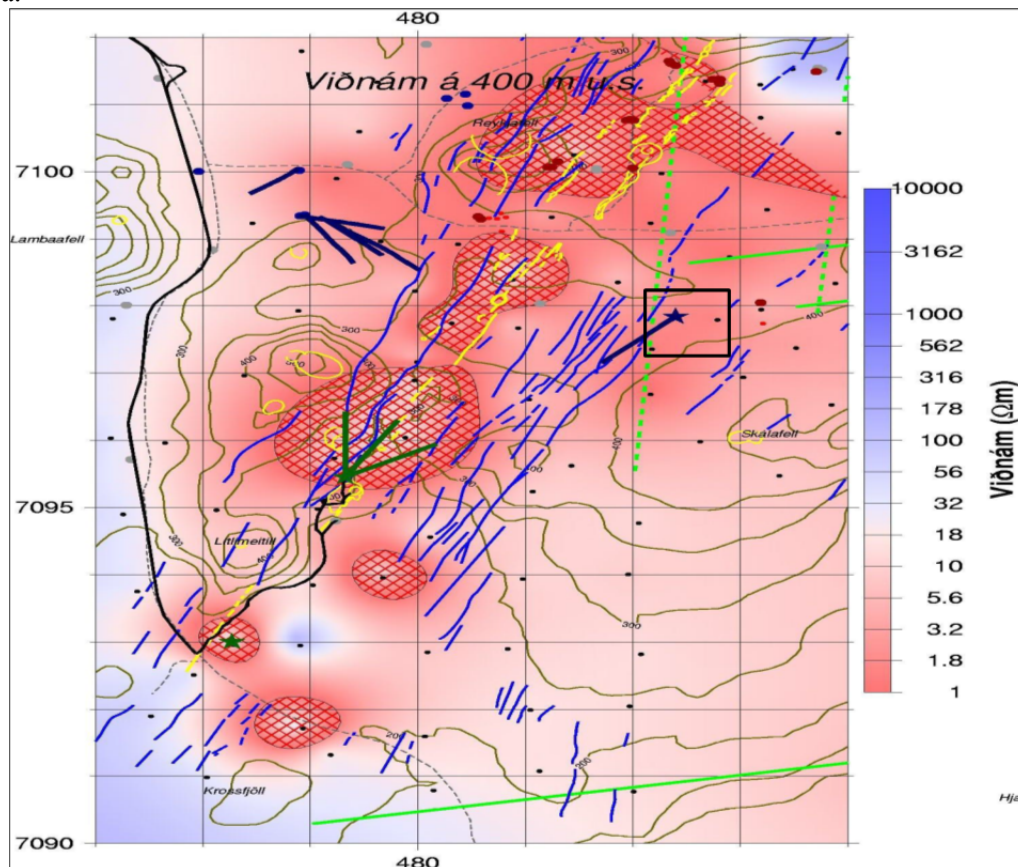


FIGURE 6: Resistivity at 400 m below sea level at Hverahlíd, Gráuhnúkar and Reykjafell (Árnason, 2007); Black rectangle approximately indicates the location of well HE-55

2. BOREHOLE GEOLOGY

2.1 Drilling well HE-55

Well HE-55 is a directional well with a total measured depth of 2782 m and is located at 383242,86 Easting and 391821,57 Northing and sits 359 m above sea level (Figures 5 and 7). The well was drilled as a multi-purpose well for exploration and production at the Hverahlíð geothermal field in the southern sector of Hengill high-temperature field. HE-55 is a slim diameter type well (Table 1) and was aimed to strike the NE-SW striking structures of the Hengill field (Figure 7). The well design is shown in Figure 8.

Drilling the well involved four phases, pre-drilling and three subsequent stages. An overview of the well and the progress of the drilling are shown in Table 1 and in Figure 9. Drilling started on May 27th, 2009 and was completed on July 29th, 2009.

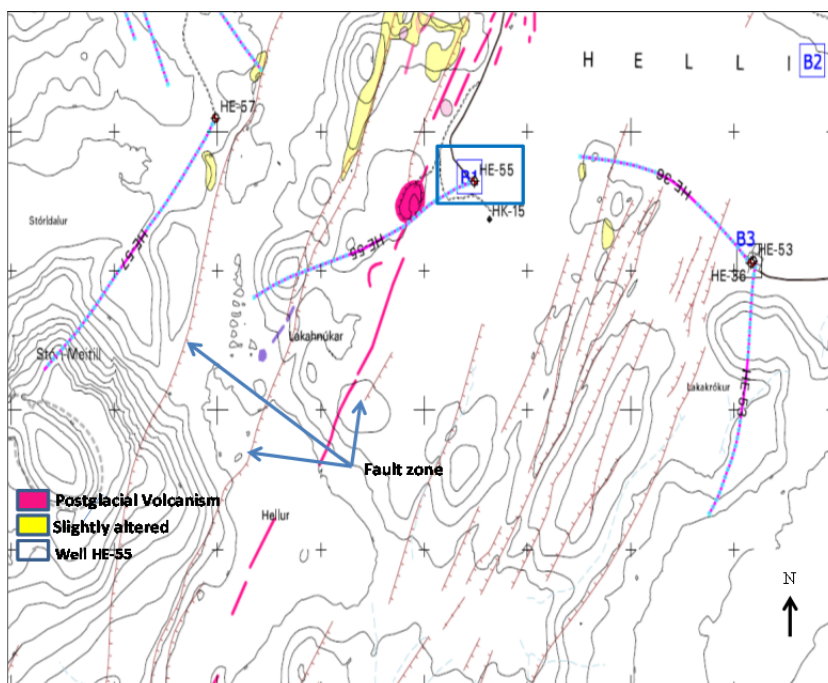


FIGURE 7: Location and direction of HE-55 extrapolated from depth to the surface according to gyro measurements (modified from a map by Iceland GeoSurvey - ISOR, unpublished)

TABLE 1: Drilling data for HE-55

Drill rig	Drilling phase	Hole size (")	Drilled depth (m)	Casing depth (m)	Casing size (")
Saga	Pre-drilling	21	97	93	18 ⁵ / ₈
Geysir	Phase one	17 ¹ / ₂	309	308	13 ³ / ₈
Geysir	Phase two	12 ¹ / ₄	810	809	9 ⁵ / ₈
Geysir	Phase three	8 ¹ / ₂	2782	697-2612	7

The first section (pre-drilling phase): From May 27th, 2009 to May 31st, 2009 using Saga drilling rig. The drilling was performed with a 21" drill bit to a depth of 97 m, and was cased with 18⁵/₈" casing to 93 m depth (Table 1). The casing was cemented in place with 8 m³ of concrete.

Phase one: Drilling of a 17¹/₂" hole, to a depth of 309 m, started on Iceland's Independence Day, June 17th, 2009, using drilling rig Geysir (Table 1). Loss of circulation of 6 l/s was encountered at 258 m, probably at the interface between two basaltic lava flows. Mica was injected which resulted in the formation gradually becoming sealed again. At 272 m depth, the loss of circulation decreased to 2 l/s and completely disappeared at 292 m depth. The drilling was completed on June 22nd at a depth of 309 m. A 13³/₈" safety casing (Table 1) was inserted in the well to a depth of 308 m. A volume of 31.3 m³ of concrete was used during cementing; subsequently, 3 m³ of cement were used for cementing through the kill-line.

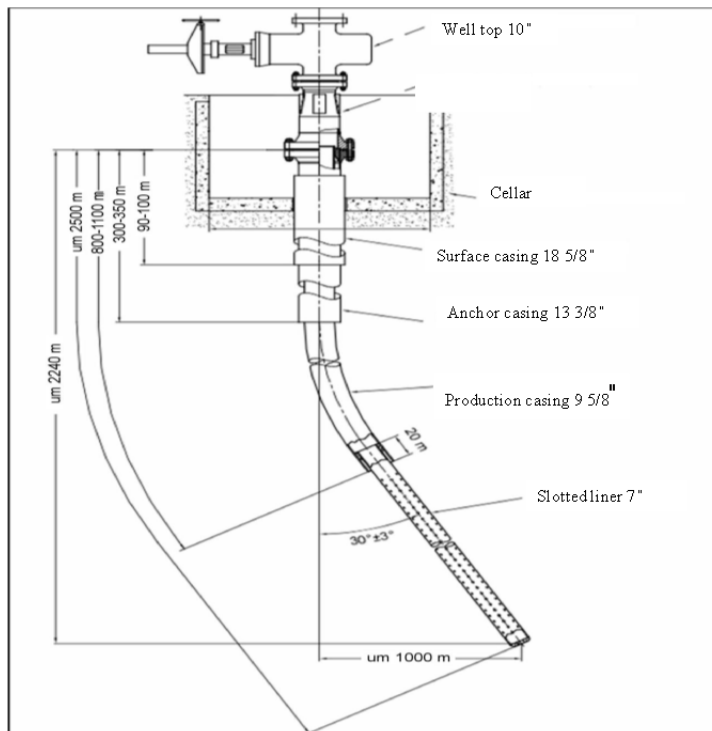


FIGURE 8: Well design of HE-55
(from Gudfinnsson et al., 2010a and b)

Phase two: The second section of the well was drilled with the same rig to a total depth of 810 m, with a 12¼" bit. In this phase the plan was to build up a dip of 30° with a bearing of 245°. Kick-off-point (KOP) was at 350 m depth and the dip was to increase close to 2.5° for every 30 m drilled. Thus, the full slope was to be reached at 710 m depth. At depth 341 m the slope and direction were measured before the initiation of deviated drilling using a MWD-instrument in the bottom hole assembly. Two gyroscopic measurements were executed on June 28th, 2009 and, as before, the building of the slope progressed very well. The depth of the well was 745 m on June 29th, 2009 at which time the slope and bearing were measured at 705 m depth, revealing that a slope of 30° had been obtained at a bearing very close to 245°. At 800 m depth, drilling slowed because of harder rock formations. At 810 m depth, the alteration mineral

assembly of the rock formations indicated that the well had reached a high-temperature system; the geologist on site decided to terminate the second phase at that point. No circulation loss was detected. The installation of a 9⅝" production casing was carried out and was retracted by 1 m so that the final depth became 809 m. A volume of 35 m³ of cement with added mica was injected through the cementing string at first, but 7.2 m³ of water was injected afterwards; an hour later, about 1.4 m³ of cement was added from the top and another 0.6 m³ half an hour later. This phase was completed after 13 workdays, on June 29th, 2009 (Figure 9).

Phase three: The third phase was drilled by the same rig to a total depth of 2782 m with an 8½" drill bit. Gyroscopic measurements on July 4th showed that the well's tilt had reduced steadily below 800 m, and was 25.6° at 947 m depth; the bearing was 243°. A new motor was put in place with a 0.8° angle. Subsequent gyroscopic measurements showed that the well had started to turn to the left below 950 m real depth but the tilt had started to build up again as planned.

Drilling continued on July 6th, 2009 and gyroscopic measurements were executed on July 7th and 8th. They showed that the well was on the correct path. At 1617 m depth, a circulation loss of 14 l/s was encountered. No fault was found and drilling resumed. At 2152 m depth, the drill bit was changed and at 2204 m the circulation loss was 20 l/s. Drilling was terminated at 2782 m, the well was cleaned and subsequently different geophysical measurements, gyro and temperature logs were carried out; the phase was completed on July 29th, 2009. The liner went down to 2612 m depth where it encountered resistance and could not go deeper, so the bottom 170 m of the well has no liner. It was decided to start pumping the well to try to stimulate it and increase permeability. At first, 65 l/s were pumped, then increased to 75 l/s and later decreased to 71 l/s.

2.2 Stratigraphy of well HE-55

In this study, the upper 1000 m of well HE-55 were analysed showing that the lithology consists of hyaloclastite formations; some crystalline basaltic lava flows and a few intrusions were also

encountered. The methods used were binocular microscope analyses, petrographic and XRD analyses, whereby the crystalline and/or textural character of the rock, which shows either porphyritic or aphyric characteristics, and the composition led to the classification of the rocks. The hyaloclastite formations contain different types of rocks such as basaltic tuff, basaltic breccias and pillow basalts (glassy basalt). The lava flows (interglacial) are fine- to medium-grained basalt or medium- to coarse-grained basalt; some fresh and compact intrusions were also encountered (Figure 10) as explained in Section 2.3. The following description of the lithology of HE-55 was achieved by using binocular and petrographical microscopes. From every 2 m of available cuttings, approximately 500 samples were analysed using binoculars; 14 thin sections were analysed using a petrographic microscope.

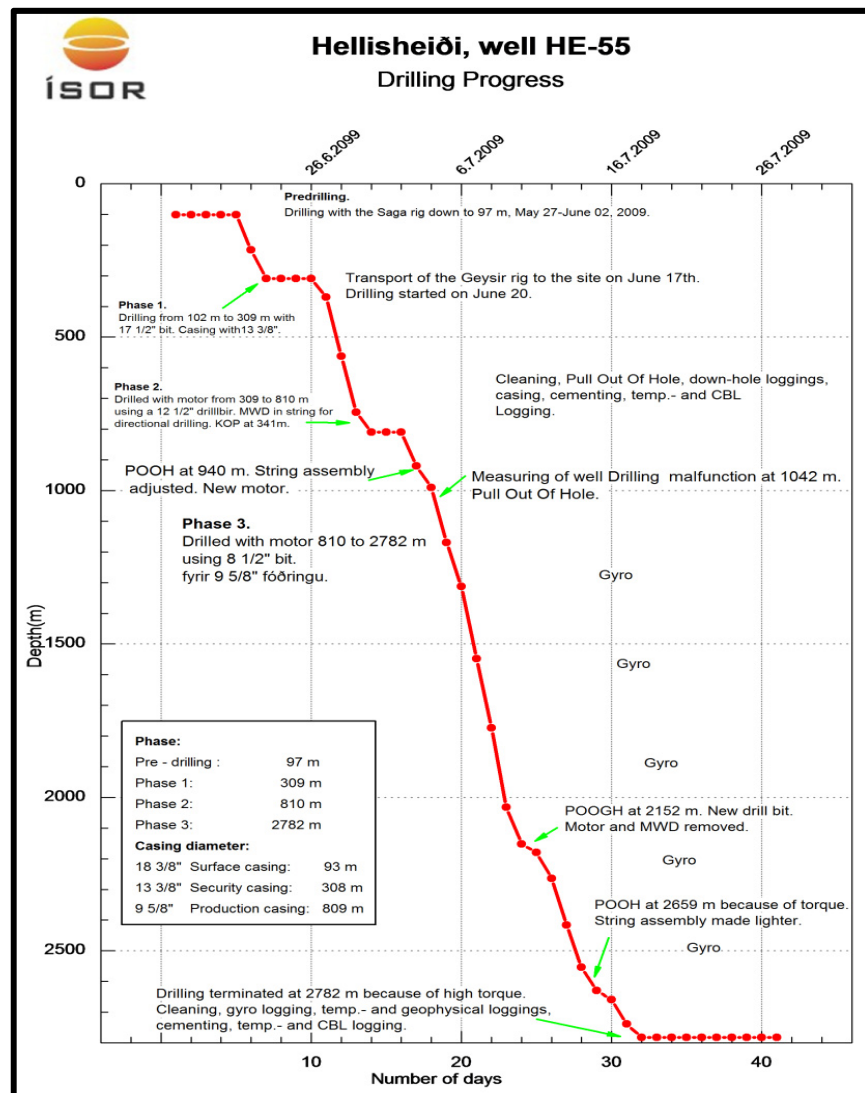


FIGURE 9: Progress of drilling stages 1, 2 and 3 of well HE-55 at Hverahlid

0 – 8 m: No cuttings

8 – 22 m: Fine- to medium-grained basalt

Light grey to dark, fine- to medium-grained basalt, less oxidized and limonite colouration present and the cuttings contain some clay materials.

22 – 95 m: Pillow basalt

Mixture of grey, fine-grained basalt fragments and black glass materials. Vesiculated basalt with olivine and plagioclase a bit oxidized. Limonite and opal observed, and the rock shows little alteration.

95 – 100 m: No cuttings

100 – 150 m: Basaltic breccia

Light grey to reddish, fine-grained basaltic breccia with olivine, plagioclase and glass. Less vesiculated and little to medium alteration. Blue mineral/opal filling vugs. At 113-114 m chabasite, siderite and analcime appear.

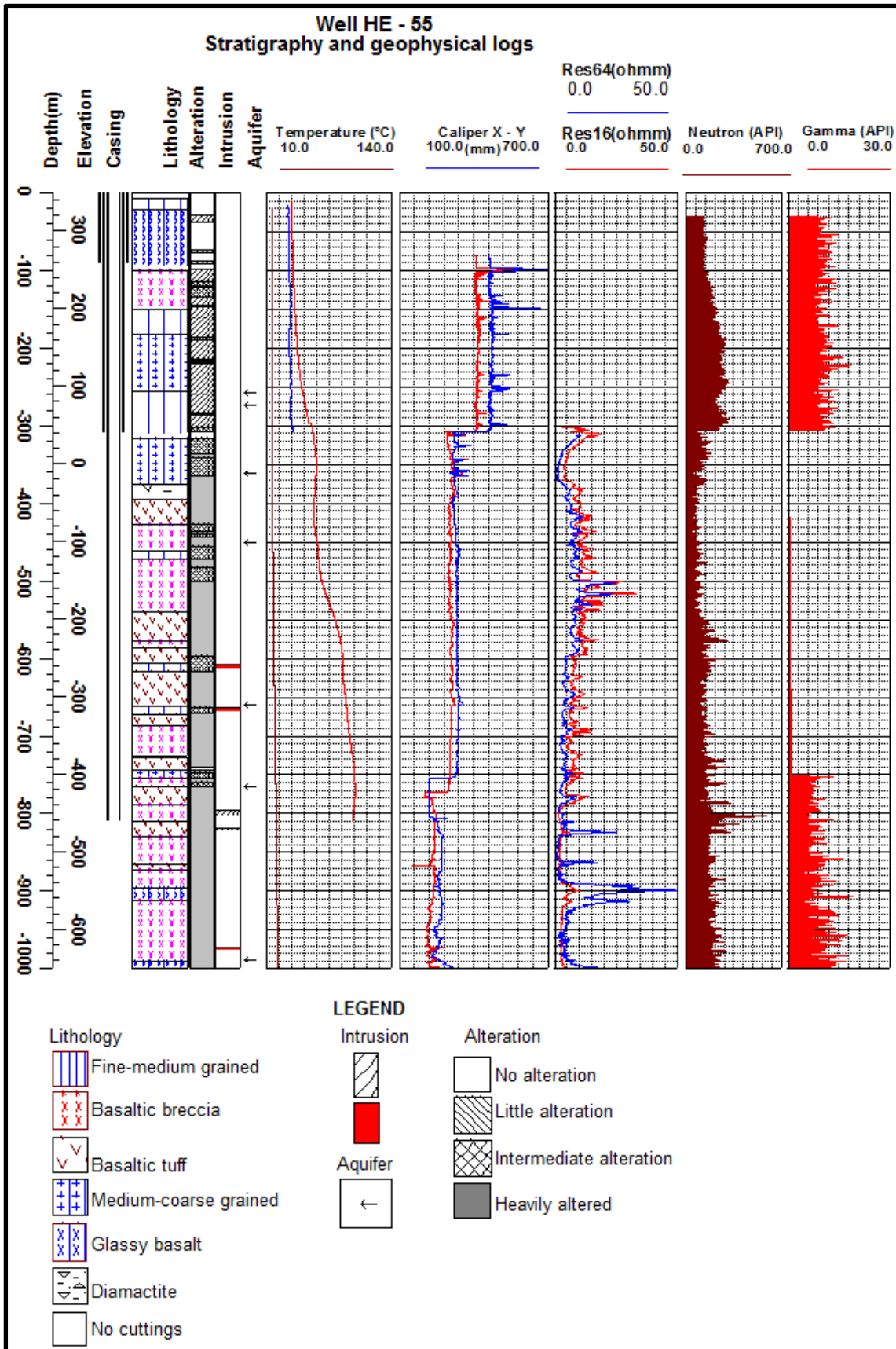


FIGURE 10: Stratigraphy, alteration stage, intrusions, feed zones and geophysical logs of well HE-55

150 – 182 m: Fine- to medium-grained basalt

Light grey, little altered, fine- to medium-grained basalt with plagioclase with some olivine and opaque minerals. Increase of calcite and pyrite is noted within the rock.

182 – 256 m: Medium- to coarse-grained basalt

Light grey coloured with white precipitates and the rock shows sub-ophitic texture. Calcite and clay minerals, especially smectite, fill vesicles. Fractured rock/veins at 199-202 m appear to be filled with pyrite and calcite. The rock is homogeneous at the bottom of this depth interval. Decreasing amount of white precipitates but increasing amount of pyrite within the rock.

256 – 309 m: Fine- to medium-grained basalt (olivine tholeiite)

Slightly altered olivine phenocrysts to clay with low precipitates. Increasing amount of calcite at the bottom and chalcedony is noted at 309 m.

309 – 316 m: No cuttings**316 – 376 m: Medium- to coarse-grained basalt**

Dark to light grey, medium-grained crystalline basalt with sub-ophitic texture and altered olivine phenocrysts. Plagioclase phenocrysts also present and a bit altered to clay minerals such as smectite which is light green to brownish. Significant amount of calcite. Quartz starts to appear at 335-336 m. Fractures are filled by calcite and clays.

376 – 396 m: Diamictite

Dark to grey, porous, fine- to coarse-grained and poorly segregated sediments mixed with medium-grained basalt fragments with some voids filled with dark clays, highly altered.

396 – 428 m: Basaltic tuff

Dark to light green to whitish altered basaltic tuffs with much calcite. Veins and/or fractures are filled by pyrite, chalcedony and clays.

428 – 462 m: Basaltic breccia

Grey to light green to whitish fine- to medium-grained rock, sub-ophitic texture, mixed with tuffs, slightly oxidized which is signified by red colouration. Plagioclase being dominant as primary mineral while pyroxene encloses plagioclase laths.

462 – 472 m: Fine- to medium-grained basalt

Light grey to darkish, fine-grained porous basalt with vugs filled with green clays. Oxidation appears and disappears within the lithology which has quartz, chalcedony and stilbite as secondary minerals.

472 – 540 m: Basaltic breccia

Highly altered basaltic breccia, seriated and aphanitic texture. The rock is mixed with some tuffs, slightly oxidized and increasing calcite, with light green to darkish clay. Fine- to coarse-grained rock with vesicles filled by clays, probably mixed layer. Chlorite starts to appear at 496 m and epidote is noted at 508 m indicating the alteration temperature might be above 230°C. At 519-520 m small spherical clusters of prehnite were noted and wairakite at 514 m.

540 – 578 m: Basaltic tuff

Light grey - whitish to greenish rock with intergranular texture, mixed with normal basaltic fragments containing plagioclase but tuffs being dominant, highly altered. Epidote encountered at 541-542 m and epidote needles, elongated, prismatic shaped start to appear at 565-566 m. Calcite is also present. Wairakite together with prehnite were observed.

578 – 586 m: Basaltic breccia

Dark grey-whitish, fine- to medium-grained rock with altered plagioclase phenocrysts. Epidote and chlorite are present, the former tending to disappear at 584-586 m. The rock is less vesiculated with epidote colouration and some tuffs are present which leads to tuffaceous basaltic breccia. The crystalline rock fragments show glomeroporphyritic texture.

586 – 606 m: Basaltic tuff

Light grey-brownish to whitish, altered basaltic tuffs occasionally vesiculated with epidote colouration mixed with fine- to medium-grained basalt fragments. White precipitates observed within the lithology and grey-bluish colour indicate the presence of clay minerals; the rock contains plagioclase and altered olivine phenocrysts.

606 – 616 m: Fine- to medium-grained basalt

Medium-altered fine- to medium-grained basalt with low oxidation at 609-614 m. Some rock fragments show compactness and massiveness with some oxidation which indicates the possibility of an intrusion.

616 – 662 m: Basaltic tuff

Light grey to green to whitish, occasionally vesiculated, medium-altered basaltic tuff with some crystalline basaltic rock but more abundant tuffs. Within this interval wairakite and prehnite exist.

662 – 672 m: Fine- to medium-grained basalt

Dark grey to whitish, intergranular texture, a mixture of basalt fragments and tuffs with plagioclase composition Fine- to medium-grained basalt with coarse-grained clay at 663-668 m and some rock fragments show the intrusion derived rock materials. Wairakite and prehnite occur together at the lower part of this depth.

672 – 686 m: Basaltic tuff

Dark-grey to green-whitish highly altered basaltic tuff with the presence of wairakite and veins filled by calcite and silica material.

686 – 726 m: Basaltic breccia

Grey to greenish, highly altered basaltic breccia mixed with light-brown to greenish basaltic tuff. The rock contains plagioclase, pyroxene, olivine and iron oxides as primary minerals. Sub-ophitic to intergranular texture.

726 – 744 m: Basaltic tuff

Light grey-greenish to whitish altered basaltic tuff with some basaltic cuttings, little oxidized with less calcite and pyrite.

744 – 754 m: Medium- to coarse-grained basaltic breccia

Dark grey-whitish, medium- to coarse-grained basaltic breccia. Low calcite but pyrite increases at first then decreases at the bottom.

754 – 766 m: Basalt breccia

Light grey-greenish to whitish medium-grained basalt with some tuffs and plagioclase being dominant as the primary mineral. The rock is less vesiculated, filled with clay and oxidized at the bottom of this section. Low calcite and pyrite are noted.

766 – 788 m: Basaltic tuff

Light brown, dark grey to whitish, altered basaltic tuff, low precipitates and rich in plagioclase. But the lithology is mixed with some slightly oxidized cuttings.

788 – 810 m: Basaltic breccia

Basaltic breccia with little vesicles, sub-ophitic texture and some tuffs are present, less oxidized. At 777-802 m there is an indication of a dyke in the fresh nature of some rock fragments of basaltic composition.

810 – 830 m: Basaltic tuff

Light green-grey tuffs with few basaltic fragments. Whitish mineral being plagioclase and epidote colouration is seen. At 819-824 m fresh fragments of a dyke containing olivine are observed.

830 – 866 m: Basaltic breccia

Light brown to greyish, fine-grained, plagioclase phyric basalt and light grey to whitish basaltic tuff with white precipitates. Decrease in pyrite and calcite.

866 – 872 m: Basaltic tuff

Light grey to greenish tuffs, dark basalt fragments, highly altered. The rock is basaltic tuff with white precipitates of calcite composition and no oxidation.

872 – 896 m: Basaltic breccia

Highly altered basaltic breccia with some prehnite and less pyrite. The crystalline rock fragments exhibit porphyritic to sub-ophitic texture.

896 – 912 m: Glassy basalt

Poorly crystallized basalt, medium- to coarse-grained, mixed with clear green tuffs. Chalcopyrite is noted rather than pyrite. Epidote appears and disappears.

912 – 990 m: Basaltic breccia

Light grey basaltic fragments, brown tuff and calcite precipitates. Highly altered, intermediate oxidized with sub-ophitic to intergranular textures. Actinolite appears at 928-930 m which indicates alteration temperatures of about 280°C, while wollastonite, epidote and chalcopyrite are noted at 945-946 m. High calcite content.

990 – 1000 m: Glassy basalt

Fine-grained poorly crystallized basalt mixed with altered glass. Quartz, clay minerals, prehnite as alteration minerals are dominant but epidote occurs at 992-996 m and 998-1000 m while wollastonite is noted at 998-1000 m. Highly altered olivine, pyroxene and plagioclase microphenocrysts and phenocrysts.

2.3 Intrusions

Intrusions are the emplacement of magma into pre-existing rock. Intrusions can be major or minor depending on their volume; a dyke is an example of a minor intrusion which is frequently fine to medium or medium to coarse grained. According to Franzson et al. (2010), the heat source at Hengill is likely to be magmatic intrusions. Dykes in the well seem to associate with oxidation due to the rapid loss of heat to the country rock, often related to permeability. Most of the dykes in well HE-55 are fine to medium grained of basaltic composition, recognized in the binocular by their compactness and a lesser degree of alteration than in the host rock. The basaltic character is recognized by low gamma values in the geophysical logs and the compactness by the resistivity and neutron logs (Figure 10). As postulated by the log plot (Figure 10), intrusions were encountered in the uppermost 1000 m of the well at 606-614, 664-668, 972-976 m, while at 796-802 and 818-822 m possible intrusions were observed. LogPlot from Rockware Inc. (2007) was used for the graphical presentation.

2.4 Interpretation of the geophysical logs

Calliper logs: The calliper log is used to reveal the presence of cavities, wash-outs and caving and can indicate the porosity state of the rock. Thus, these logs can be used to identify fractures and possible water-producing or receiving zones and to correct other geophysical logs for changes in the borehole diameter (Senior et al., 2005). From Figure 10, two peaks correspond to circulation losses at 258 and 274 m, indicating a permeable zone and/or water receiving zone. In addition, calliper logs are used to calculate the volume of cement needed for casings.

Temperature logs: Temperature logs are used to identify possible aquifers and are usually carried out during and after drilling. The water flowing in or out of the well tends to affect temperature by increasing or decreasing the temperature. In well HE-55, temperature logs indicate aquifers at 258, 274, 362, 450, 660, 765 and 988 m.

Resistivity logs: Two things are described by the resistivity of a rock: the formation fluid and the resistivity of the rock matrix. The two resistivities contribute to the specific resistivity of the reservoir rock. According to Mostaghel (1999), an igneous rock matrix is generally a poor electrical conductor at geothermal temperatures. Consequently, rocks having prominent vesicles/and or cavities will show low resistivity values (Figure 10).

Neutron – neutron logs: The quantity of hydrogen in a rock formation is observed as variations in the neutron-neutron logs. Values can be high or low; the latter indicates the water content in the formation, which practically is the potential source of hydrogen. If liquid rich in hydrogen fills the pore volume, then one can use hydrogen richness as an index to porosity. In HE-55, high peaks indicating low water content (relatively fresh rocks) are observed at 284, 578, 762, and 982 m.

Gamma logs: Natural gamma radiation is often used to determine the clay content in rocks. Investigations in Iceland show, however, that the gamma ray activity in volcanic rocks is related to the SiO₂ content of the rock and can, therefore, be used to identify rocks of evolved compositions (Mostaghel, 1999). The gamma results showed low values in the fresh rocks and a general increase in the alteration zone. Gamma logs in HE-55 did not indicate the presence of rocks of evolved compositions (Figure 10).

2.5 Hydrothermal alteration

Hydrothermal alteration is the response of the rock, in terms of mineralogical, textural and chemical alterations, when subjected to thermal environments in the presence of hot water and gas. Identifying hydrothermal alteration is crucial in both geothermal and ore-deposit exploration. In geothermal systems, hydrothermal alteration can reveal the history, and possibly the future, of the system involved. In addition, hydrothermal minerals are useful geothermometers and are used, for example, to assist in determining the depth of production casing during drilling. Hydrothermal minerals are also used to determine the alteration temperatures of wells and, when compared to formation temperatures, can predict whether the rock formations in a specific area are cooling or heating. Hydrothermal minerals can also be used in estimating fluid pH and other chemical parameters, as well as predicting scaling and corrosion tendencies of fluids, measuring permeability, possible cold-water influx and as a guide to the hydrology (Reyes, 1990).

When the rock heats up, especially in active volcanic areas, then the rock will release some ions into the solution. This hydrothermal solution, after undergoing further heating, will rise up as a mineral rich fluid. The mineral rich fluid will tend to crystallize out of the solution onto open cavities and/or open structures depending on temperature, rock type, pressure, permeability, fluid composition and duration of activity. For example, epidote starts to appear at about 230°C and exists to over 300°C

(Kristmannsdóttir, 1979; Franzson, 1998). Figure 11 shows the mineral alteration zones in Iceland vs. temperature.

2.5.1 Analytical methods

Binocular microscope

Drill cuttings were sampled at an interval of 2 m if possible, as some depths had no cuttings due to circulation losses. The samples were mounted on a binocular microscope to analyze different features such as rock type(s), grain size, oxidation, alteration minerals, primary minerals and alteration stage.

Petrographic microscope

The petrographic analyses were based on 14 thin sections from the uppermost 1000 m of HE-55. Thin sections were selected from different depths. The aim

was to confirm rock type(s), texture, porosity and alteration minerals, additional minerals not observed by the binocular, and to study the mineralogical depositional sequences of secondary minerals.

XRD analysis

The samples were placed in crucibles, 1/5 sample then 3/4 water and subsequently shaken for 4 hrs in a shaker machine to separate the phyllo-silicates from the rock matrix. When finished, the samples were mounted on glass, dried and were then ready for XRD-analysis. This method is very important for identifying clays and zeolites, which in turn provide information on alteration temperatures. The XRD analyses of clay minerals in HE-55 are found in Appendices I and II.

2.5.2 Primary rock minerals in HE-55

Primary minerals are rock forming minerals which are formed at the same time as the host rock. Primary minerals crystallize from magma, governed by the physico-chemical conditions under which the magma solidifies (e.g. Njue, 2010). They alter to secondary minerals under certain conditions where there is high permeability, elevated temperatures and intense fluid activity particularly in geothermal environments. Secondary minerals form via chemical reactions between primary minerals and hydrothermal fluids. As described earlier in Section 1.2, the geology of Iceland is composed of igneous rocks of which about 80-85% are basaltic in composition. The main primary minerals, in order of their susceptibility to alteration, are:

1. Glass (amorphous, quenched liquid);
2. Olivine;
3. Plagioclase;
4. Pyroxene;
5. Opaques.

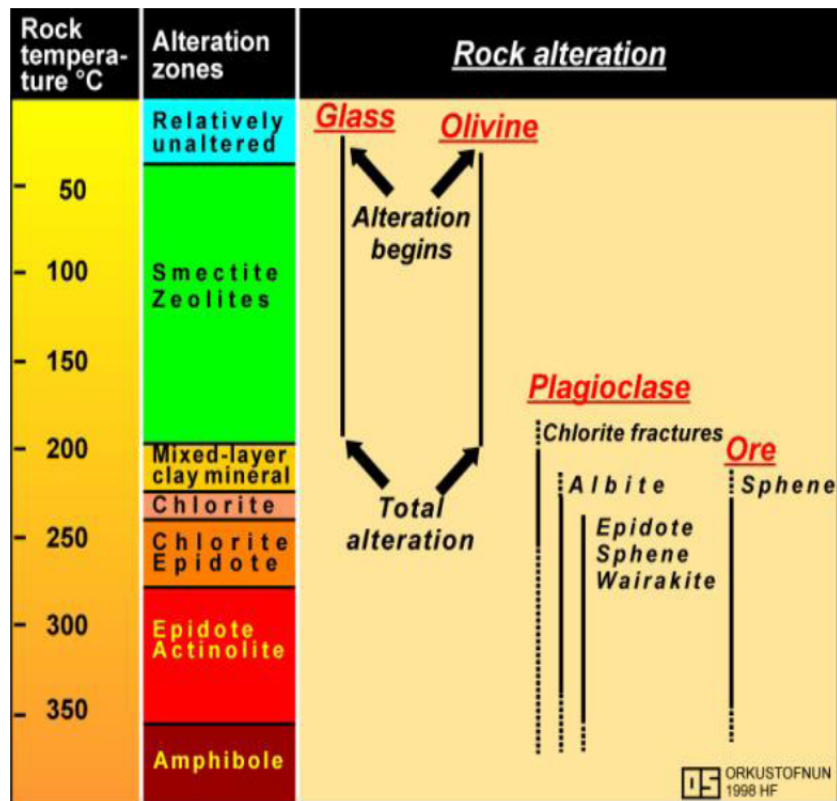


FIGURE 11: Mineral alteration vs. temperature diagram (slightly modified from Franzson, 2011)


Volcanic glass: It is amorphous quenched magma and shows a highly vitreous lustre and has good conchoidal fractures. It is the first constituent to be altered and replaced (Table 2). The replacement products of volcanic glass are zeolites (mordenite, laumontite), cristobalite, quartz, calcite and clays (Browne, 1978).

Olivine: It is one of the primary minerals that forms basaltic rocks (e.g. olivine tholeiite) and is very susceptible to alteration. It is distinguished in thin section by its high birefringence, distinctive irregular fracture pattern, lack of cleavage, and alteration products, usually clay, forming along rims and fractures. It is completely replaced by calcite and clay at depth.

Plagioclase: It is the most abundant mineral occurring in most igneous rocks. In crystalline rocks it is readily identified by its low relief and conspicuous polysynthetic twinning. The untwined plagioclase (albite), which resembles quartz, shows incipient alteration or clouding which is not common in quartz. It also occurs as a fine groundmass in rocks exhibiting porphyritic textures. It is observed to be progressively altered as temperature increases and is finally replaced by albite and occasionally by calcite, wairakite, chlorite and epidote.

Pyroxene: The dominant pyroxenes that occur in Icelandic basalts are the clinopyroxenes, occurring as phenocrysts and in the groundmass. The pyroxenes resemble olivine but differ by the presence of better cleavage and inclined extinction. Pyroxene is observed to alter to clay as well as to actinolite at higher temperatures.

TABLE 2: Primary rock minerals and their alteration products in well HE-55

Susceptibility	Primary rock minerals	Alteration mineral results
	Glass Olivine Plagioclase Pyroxene Opaque	Clay, zeolite, calcite, quartz Clay, calcite, quartz Clay, calcite, albite, quartz, wairakite, chlorite, epidote Clay, actinolite Sulphides

2.5.3 Hydrothermal minerals of well HE-55

In HE-55, different hydrothermal minerals were observed but the most common minerals in the upper 1000 m were clays, quartz, pyrite, calcite and zeolites. Hydrothermal minerals are formed as a result of the alteration of primary minerals such as glass, olivine, plagioclase, pyroxene and opaque minerals and can occur due to hydrothermal deposition. Geothermal systems always associate with H₂S and CO₂ which contribute to the availability of calcite and pyrite, but pyrite seems to grow into chalcopyrite. The probable cause of the abundance of calcite and pyrite is the H₂S and CO₂ content commonly associated with geothermal systems. The distribution of alteration minerals with depth in well HE-55 is shown in Figure 12, and the different minerals are described here below:

Limonite: This mineral is characterized by a reddish brown colour; it is hydrated iron oxide and is formed due to the interaction of rocks with cold groundwater. It is present in the well at 10 m down to 250 m within different rock formations.

Siderite is a hexagonal iron carbonate with curved and striated faces; it occurs with limonite and belongs to the calcite group of carbonates. In the cuttings, aggregates of siderite appeared to fill vugs, starting at 114 m and disappearing at 136 m in well HE-55.

Zeolites: These are secondary minerals which are hydrous sodium calcium aluminium silicates occurring by filling cavities in rocks. In nature, zeolites are temperature dependent which can help in determining the temperature at a given depth in geothermal systems. There are over 40 naturally

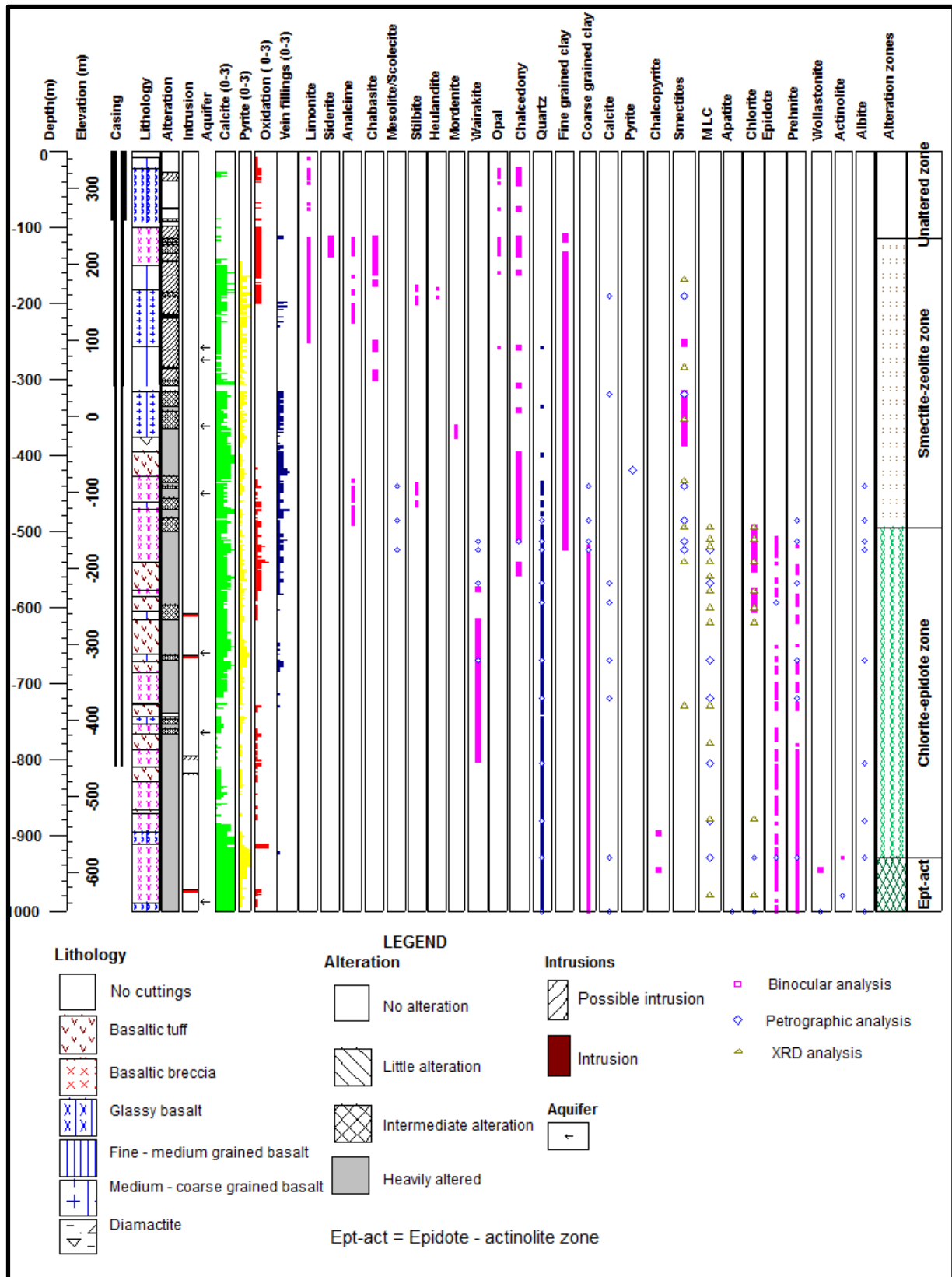


FIGURE 12: Lithology, distribution of hydrothermal minerals and alteration zones in the upper most 1000 m of well HE-55

occurring zeolites which are often classified, according to shape, in three main categories: fibrous/acicular, tabular/prismatic, and granular (e.g. Kristmannsdóttir, 1979; Koestono, 2007). The following types of zeolites were found in the well:

Analcime: It was found at depths from 114 to 488 m, indicating temperatures between 40 and 60°C. Occurs as cube crystals in a similar way to wairakite.

Mesolite/scolecite: Scolecite occurs as radiating structures (Figure 13) in thin section, but mesolite is light in colour; the two can be classified as fibrous/ acicular. Both occur at around 90°C and were observed at 440, 486 and 524 m.

Chabasite: It is stable from about 30 to about 80°C; it is cubic through binocular, appears white to clear and belongs to the tabular category of zeolites. In the well, it occurs at 114-298 m.

Stilbite: This indicates temperatures between 90 and 120°C. It is white to clear in binocular. In HE-55, it was first noted at 178 m and last observed at 462 m.

Heulandite: The mineral has a tabular and a bit radial form with a lustrous reflection; it was encountered at 180 and 192 m. The mineral signifies temperatures between 90 and 150°C.

Mordenite: Is a zeolite with orthorhombic structure and crystallizes in fibrous aggregates with a striated prismatic shape. It is colourless, white or pink. The well formed mordenite develops hairlike crystals; the mineral was noted below 362 m. It occurs at temperatures above 90°C.

Wairakite: Formation of wairakite is seen between 524 and 790 m. Wairakite appears transparent and has a very low birefringence. It also shows box-like structures in thin section. The mineral indicates temperatures greater than 200°C.

Opal: It was found between 24 and 258 m indicating temperatures below 100°C. In cuttings, it looks pale yellow-brown in colour and tends to fill cavities/vugs and can be replaced/altered to quartz.

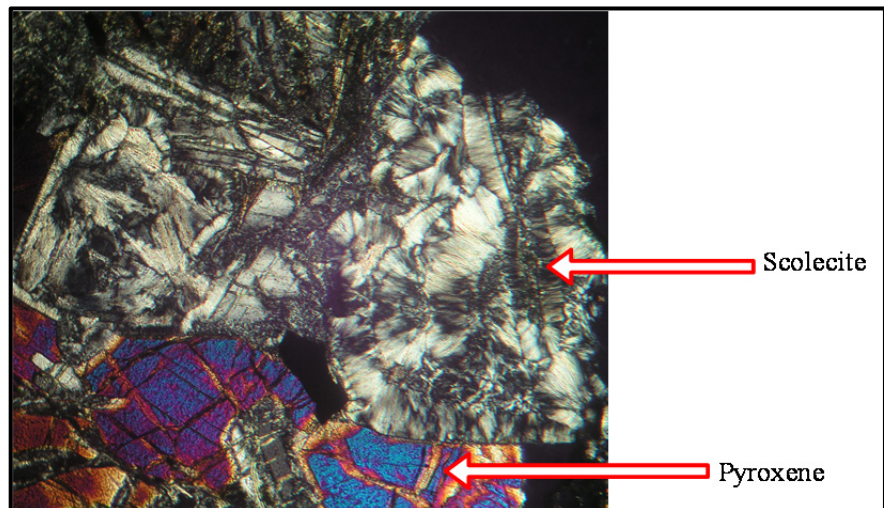


FIGURE 13: Photo showing scolecite and pyroxene

Chalcedony: Chalcedony exhibits a bluish colour under the binocular microscope and seems to fill vesicles evenly; it is a low-temperature silica mineral. It was noted from 160 to 556 m. Chalcedony can be replaced/altered to quartz.

Quartz: Binocular and petrographic analyses show quartz deposits in vugs and veins. Secondary quartz forms at temperatures of above 180°C. In cuttings it showed an euhedral shape. Quartz in thin section appears with no clear twinning but with a highly refractive index; the latter can be used to distinguish quartz from zeolites. Quartz is stable in a geothermal system and can be used as an indicator mineral for production casing if it shows a clear prismatic shape.

Fine-grained clay: Can be identified under the petrographic microscope as fine layers, mostly composed of smectite and mixed-layer clays. Fine-grained clay forms at lower temperatures than coarse-grained clay.

Coarse-grained clay: Coarse-grained clay forms fibrous structures which can be differentiated from fine-grained clay. In cases where the fine- and coarse-grained clays occur together, the latter overlaps the former as they are formed later.

Prehnite: The mineral in the well forms below 486 m depth and occurs together with wairakite; the temperature for prehnite is above 240°C. The bow tie structure of prehnite is clearly identified in thin sections as is its high interference colour and high relief.

Epidote: The yellow to green colour stands out as a distinctive feature of epidote. The mineral was first noted at 508 m but the crystals occur occasionally later. Crystals with prismatic shape become prominent at 832 m. It was found to associate with quartz in HE-55. The mineral has a strong pleochroism of green, yellow and brown in thin section. The occurrence of epidote indicates temperatures above 230°C (e.g. Kristmannsdóttir, 1979) and is an important mineral when deciding the depth for production casing.

Wollastonite: Occurrence temperature for wollastonite is about 270°C; it can associate with epidote and garnet; in HE-55, it is associated with epidote. It is rare in well HE-55, but was identified in a cutting at 946 m by its hair-like structure. In thin section it shows weak birefringence and has a fairly high relief.

Calcite: Calcite is the most abundant mineral in the well, appearing from 30 m; hydrochloric acid was used to identify it in cuttings. It was seen all the way to the bottom of the well. Calcite formation can be linked to boiling, dilution and condensation of carbon dioxide in a geothermal system. It can also form during the heating of cooler peripheral fluids (Simmons and Christenson, 1994). Calcite crystals have clear cleavage and high interference colour in thin section and can be distinguished from plagioclase by these properties. Also, calcite occurs over a wide temperature range and replaces calcium bearing minerals such as plagioclase, zeolite and glass in the presence of CO₂-rich fluids in rocks with low porosity and permeability. In open spaces, calcite deposits in response to boiling (Thompson and Thompson, 1996). In thin section, radial, platy and dog tooth-like structures were observed. In well HE-55, calcite occurs as vein and vesicle fillings.

Pyrite: The mineral forms yellowish cubic crystals and is abundant in HE-55 samples below 148 m. Pyrite in a geothermal system can be used as an indication of permeability. In HE-55, it is disseminated and fills veins/vugs.

Chalcopyrite: It is a brassy/golden yellow tetragonal mineral and occurs in association with pyrite. The mineral was noted at 898 and 946 m.

Albite: The mineral occurs as an alteration product of plagioclase although it is also perceived to precipitate in some vesicles. Albite was noted at 486 m where it replaces plagioclase; it tends to destroy the characteristic plagioclase twinning habit.

Actinolite: The pale green coloured prismatic habit of the mineral was observed through binocular at 930 and 980 m. The mineral forms at temperatures above 280°C (Franzson, 2011).

Clay minerals: These are water-rich phyllosilicates that form by hydrous alteration of primary silicate minerals such as glass, plagioclase, pyroxene, olivine and pyroxene. The composition, structure and morphology of clay minerals depend on a number of environmental parameters, such as temperature, fluid composition/amount, pH, etc. Clay crystals are finely crystalline or meta-colloidal and occur in flake-like or dense aggregates of varying types (Ahmed, 2008). Clay minerals are identified easily by XRD analysis but also with petrographic analysis and binocular microscope. Clays are classified into different types and tend to occur at different depths according to temperature (Figure 14).

Clay minerals were analysed using the binocular microscope, petrographic microscope and XRD analysis; the identified clay zones are narrated below.

Smectite zone: In XRD it was identified between 170 and 780 m. The peak values of the untreated samples showed values of 13.66-7.47 Å, but 13.70-17.67 Å for glycolated samples; the heated sample value was 10 Å. Smectite indicates a temperature of approximately 200°C. In petrographic analysis, smectite was noted at 252 m, appearing brownish and having low birefringence, mostly filling vesicles.

Mixed-layer clay: The clay is strongly pleochroic with low birefringence; it was noted at 524 m in thin section, occurring in multiple layers from fine- to coarse-grained clay layers. From XRD analysis, mixed-layer clays were noted at 496-980 m, shown by peak characteristics of both smectite and chlorite. Smectite showed a collapsed character when heated and chlorite showed peaks at about 7 and 14 Å.

Chlorite: The presence of chlorite indicates temperatures of above 230°C as chlorite has a crystallization temperature of over 230°C (Franzson, 1998). Under petrographic analysis, the mineral appears green and non-pleochroic in plane polarized light; under crossed polars it is dark green to brown. In binocular, chlorite appears green and was noted at 496 m. In XRD analysis, chlorite was identified with peaks at 14.88 and 7.74 Å.

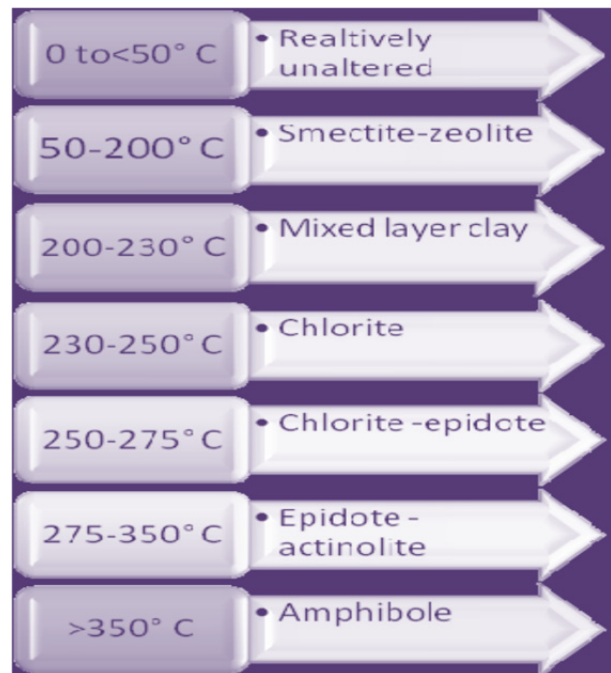


FIGURE 14: Alteration zones in the high-temperature geothermal fields in Iceland (modified from Franzson, 2011)

2.5.4 Alteration mineral zonation

Results from binocular, petrographic and XRD analysis made it possible to define three alteration mineral zones in the top 1000 m of HE-55. The zones were revealed by considering the alteration mineral temperatures and abundance. In the Icelandic geothermal settings, low-temperature zeolites and amorphous silica form below 100°C, chalcedony below 180°C, quartz above 180°C, wairakite above 200°C, epidote above 240°C and garnet and amphibole above 280°C (Kristmannsdóttir, 1979; Saemundsson and Gunnlaugsson, 2002; Franzson, 1998). The temperature range in low-temperature geothermal areas is well within the uppermost alteration zone of the high-temperature geothermal areas (Kristmannsdóttir, 1975). For the clay minerals smectite crystallizes below 200°C, mixed-layer clays at 200-230°C and chlorite above 230°C (Kristmannsdóttir, 1977). Figure 14 shows alteration zones in high-temperature geothermal fields in Iceland.

During the study of HE-55 down to 1000 m, the boundary between one zone and another was defined by the first appearance of the successive dominant alteration mineral (Figure 12).

Unaltered zone (0 – 114 m): A relatively unaltered zone indicated by minerals which form even in cold groundwater. The zone is signified by low-temperature minerals from 0 to 50°C.

Smectite – zeolite zone (114 – 496 m): The occurrence of smectite at 190 m by petrographic analysis and the presence of zeolites were used to indicate this zone. Within this zone, the minerals indicates temperatures of 50-200°C.

Chlorite – epidote zone (496 – 930 m): Epidote, the yellow–green mineral, was first noted at 508 m in the cuttings and chlorite was noted at 496 m; the zone indicates temperatures of 250-275°C.

Epidote – actinolite (930 – 1000 m): Actinolite marks the upper boundary of this zone and was identified under the binocular at 930 m; the mineral assemblage indicates temperatures of 275-350°C.

3. AQUIFERS/FEED ZONES

Aquifers are underground layers of water-bearing permeable rock or unconsolidated materials (e.g. Alnethary, 2010). In well HE-55, feed zones/aquifers were located by considering the following:

- Geophysical logs such as temperature, calliper, etc.;
- Circulation losses;
- Hydrothermal alteration;
- Other drilling data such as the variation in the penetration rate, pressure changes during drilling and circulating fluid temperatures.

At least some of the aquifers encountered in the wells can be directly related to lithological boundaries and margins of intrusions, indicating the presence of fracture permeability in the geothermal reservoir (Figures 10 and 15). The rock, which is rich in vein/vesicle networks and has a high concentration of hydrothermal minerals, is an indication of the presence of strong subsurface hydrological circulation. Alteration minerals such as crystallized quartz, adularia, anhydrite, wairakite, illite, hyalophane, abundant pyrite and calcite are also positive signs of good permeability. However, the absence of these alteration minerals, a low degree of alteration, the precipitation of prehnite, pumpellyite, pyrrhotite and large quantities of laumontite and titanite can be attributed to a low-permeability zone (Reyes, 2000).

Seven separate aquifers were identified, at 258, 274, 362, 450, 660, 765 and 988 m.

Aquifers 1 and 2: These feed zones are at 258 and 274 m and were identified by circulation loss, and an increase in temperature at 258-274 m. The former is approximately at the boundary of medium- to coarse-grained basalt and a fine- to medium-grained basalt (olivine tholeiite) formation. Both the formations are intermediate in alteration. The latter aquifer is hosted by olivine tholeiite. Circulation losses were about 6 and 2 l/s, respectively. Increased amounts of calcite and pyrite were seen.

Aquifer 3: This aquifer is at 362 m, indicated by an increase in the temperature log, high peak in the caliper log, low resistivity and a low peak in the neutron log (Figures 10 and 15).

Aquifer 4: The feed zone is vertical and located at 450 m in basaltic breccia, highly altered rock; the aquifer was realized by a decrease in the temperature log and a low-resistivity peak (Figures 10 and 15).

Aquifer 5: The feed zone is at the margin of an intrusion at 660 m; an increase in the temperature log with low resistivity and a change in the rate of penetration were observed. It is in the chlorite zone and located in basaltic tuff (Figures 10 and 15).

Aquifer 6: It is at the boundary of basaltic tuff and basaltic breccia at 765 m. At this depth, low resistivity was observed along with a slight increase in the temperature log and a low peak in the gamma log. Less calcite and pyrite were deposited (Figures 10 and 15).

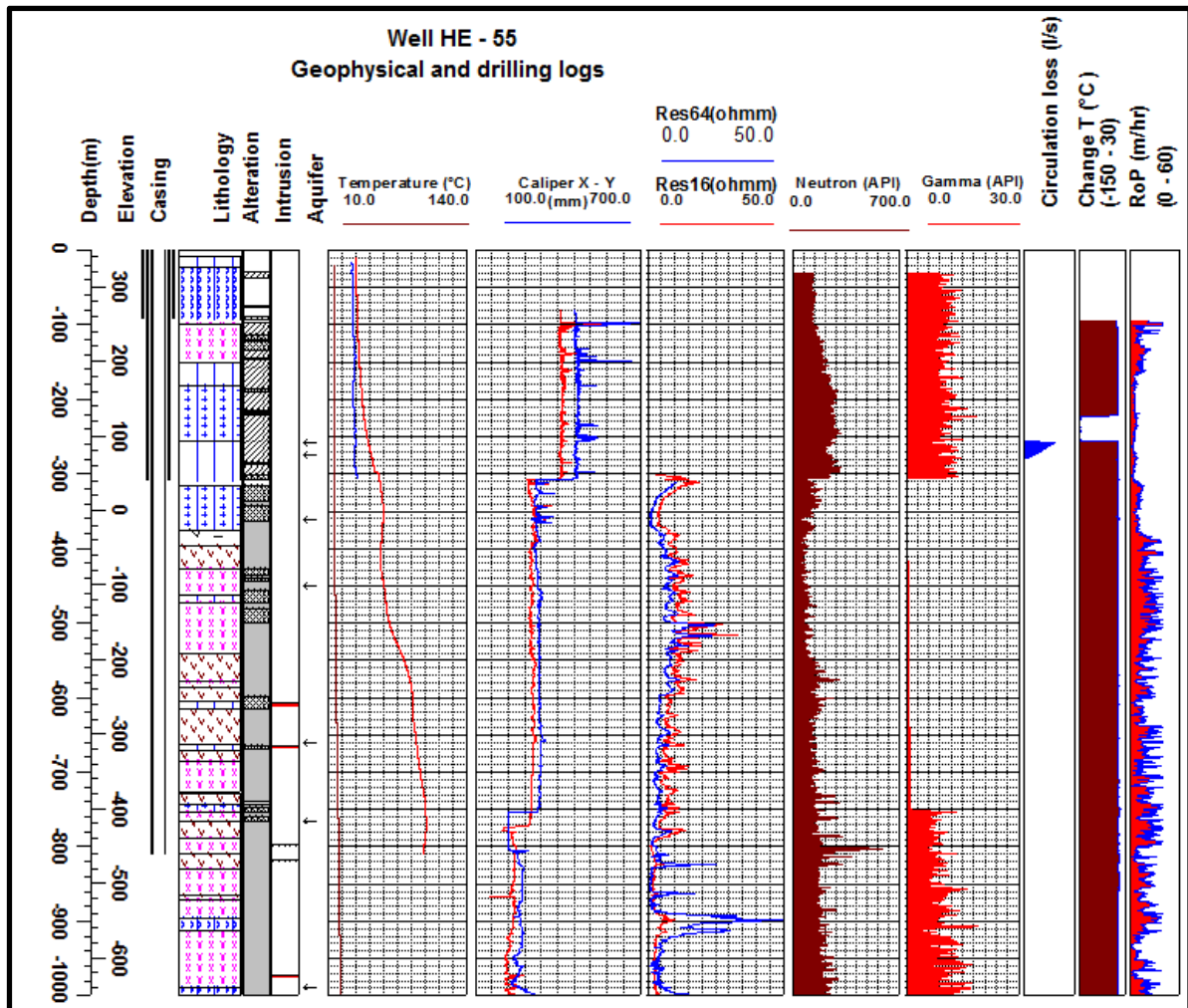


FIGURE 15: Geophysical logs and some drilling logs from well HE-55; gamma logs are missing between 306.2 and 750.5 m

Aquifer 7: It is found at 988 m, indicated by a high peak in the calliper log which indicates porosity/permeability; the gamma log showed low values at that depth (Figures 10 and 15). Highly altered basaltic breccia was seen with significant calcite formation, indicating permeability.

4. VEINS AND VESICLE FILLINGS IN WELL HE-55

Veins are micro-fractures that are filled up either by fluid or with the deposition of secondary minerals. Vesicles, on the other hand, are pore spaces. Despite the difference in structure, both are very important, not only as sources of permeability, but also as 'sample holders'. Hydrothermal alteration minerals, known to be very important geothermometers, deposit within these structures and must be carefully studied, using both binocular and petrographic analyses. Basically, porosity and permeability are two of the primary factors that control the movement and storage of fluids in rocks and lead to the deposition of minerals either in veins or vesicles (e.g. Gebrehiwot, 2010).

In well HE-55, vesicles and veins were encountered at different depths, but most were vesicles. These veins and vesicles were sometimes filled by zeolites, calcite, pyrite, quartz, clay, wairakite, prehnite and epidote. However, some vesicles were clear of any alteration products. The mineral fillings were identified by binocular microscope and petrographic analysis. Veins and vesicles can be used as a special tool for determining mineral deposition sequences.

5. MINERAL DEPOSITION SEQUENCES IN WELL HE-55

Mineral deposition sequences depend on specific evolution and reactions regarding various factors such as temperature, fluid composition, rock type, the interaction between the hydrothermal fluids and the host rock, porosity, permeability and the duration of the interactions. Many of the minerals are formed as replacement minerals, via alteration or by deposition; by studying their depositional sequences in veins and vesicles, one can explore the parent thermal history and relative time scale of alteration minerals within a geothermal system (e.g. Mbia, 2010).

The secondary hydrothermal mineralization and the mineral deposition sequences in well HE-55 were identified using a petrographic microscope; the results are given in Table 3. Most of the minerals were deposited in vesicles and veins, the older coming first, followed by the younger.

TABLE 3: Time sequence of alteration mineral deposition in the uppermost 1000 m of well HE-55

Lithology	Depth (m)	Alteration	Older → → → Younger
Medium to coarse grained basalt	190	Intermediate	S ₁ : Glassy → Smectite S ₂ : Smectite → Calcite
Medium-coarse grained basalt	320	Intermediate	Smectite → Calcite
Basaltic breccia	440	Heavily	Smectite → Coarse grained clay → Calcite
Basaltic breccia	486	Intermediate	S ₁ : Smectite → Calcite → Quartz S ₂ : Smectite → Coarse grained clay → Quartz → Prehnite
Basaltic breccia	514	Heavily	Smectite → Calcite → Chalcedony
Basaltic breccia	524	Heavily	Mixed Layer Clay → Calcite → Quartz
Basaltic tuff	568	Heavily	S ₁ : Calcite → Quartz S ₂ : Mixed Layer Clay → Quartz
Basaltic tuff	594	Heavily	-
Fine-medium grained basalt	670	Intermediate	Mixed Layer Clay → Quartz → Wairakite → Prehnite
Basaltic breccia	720	Heavily	Mixed Layer Clay → Quartz → Prehnite
Basaltic breccia	806	Heavily	Mixed Layer Clay → Quartz
Basaltic breccia	882	Heavily	Mixed Layer Clay → Prehnite → Quartz
Tuffaceous basaltic breccia	930	Heavily	S ₁ : Calcite → Quartz → Epidote S ₁ : Mixed Layer Clay → Quartz → Calcite
Glassy basalt	1000	Heavily	Calcite → Quartz → Chlorite

S₁ - Sequence 1, S₂ - Sequence

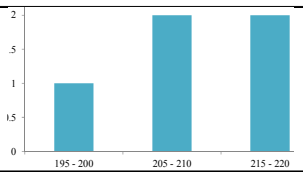
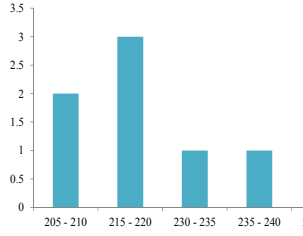
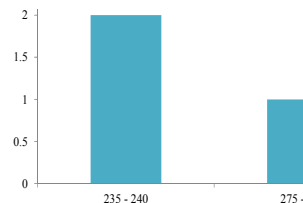
Different minerals were identified; calcite, mixed-layer clay and quartz were dominant. In Table 3, the arrow points to the younger, for example, at 720 m the sequence shows that the system is heating, with alteration changing from a low-temperature to a high temperature alteration mineral. At 930 m, sequence 1 (S₁) (Table 3) shows that calcite occurs after quartz; the appearance of calcite at a later stage in the high-temperature mineral sequence may indicate cooling of the system.

6. FLUID INCLUSIONS

Fluid inclusions are a tool which is used to predict whether a geothermal system is cooling or heating and consequently may allow us to interpret the history of the system. Fluid inclusions occur when hydrothermal minerals are growing or crystallizing in a fluid environment, whereby a small cavity/vug tends to trap small amounts of fluid which will lead to primary fluid inclusion. Secondary inclusions are formed during re-crystallisation, provided there are micro-fractures present. Heating crystals which contain fluid inclusions provides the homogenization temperatures which are plotted in histograms. Fluid inclusion histograms are plotted with formation temperatures, alteration mineral temperatures and boiling temperature curves in order to establish whether a geothermal system is heating or cooling. Formation temperatures used in this report may be slightly lower than found in the present natural system as water was periodically pumped into the well after its completion to enhance permeability and may have affected the heating-up temperature logs.

Alteration minerals containing fluid inclusions in well HE-55 were sampled at depth intervals 746-760, 1090-1104 and 2108-2124 m. For the first depth, only one calcite crystal was analysed; it had 5 fluid inclusions. For the second depth, two calcite crystals were found with nine fluid inclusions. The third depth had one calcite crystal with three fluid inclusions. A total of 17 fluid inclusions were analysed, most of them being secondary (Table 4).

TABLE 4: Homogenization temperatures, depth, frequency and corresponding histograms

Depth (m)	Crystal	Fluid inclusion temperature ranges (°C)	Frequency	Histogram X = (°C) Y = Frequency
746 – 760	Calcite	195 – 200 205 - 210 215 - 220	1 2 2	
1090 - 1104	Calcite 2 1 1 2 1	205 – 210 215 – 220 230 – 235 235 – 240 280 - 285	2 3 1 2 1	
2108 - 2124	Calcite 1 1	235 - 240 275 - 280	2 1	
Total of 17 Fluid Inclusions				

In the depth range of 746-760 m, homogenization temperatures of most inclusions were between 195 and 220°C, overlapping the formation temperatures, which indicates that the system was in equilibrium with the inclusions as they formed (Figure 16). However, only one crystal was analysed and the alteration mineral temperatures was higher than the formation temperature, indicating cooling. From 1090-1104 m, homogenization temperatures of most inclusions were between 210 and 240°C, but the homogenization temperature of two inclusions was 280-285°C. The last depth, 2108-2124 m showed homogenization temperatures ranging between 235 and 280°C (Figure 16).

At depths 1090-1104, the homogenization temperatures of the fluid inclusions were outside the formation temperature curve and, by being higher, indicated cooling of the system which is, thus, not in equilibrium. Results from the depth range 2108-2124 m showed that the homogenization temperature was higher and did not overlap with the formation temperature; consequently, it can be assumed that the geothermal system was cooling at that depth (Figure 16). The fluid inclusions in HE-55 generally indicate cooling of the system.

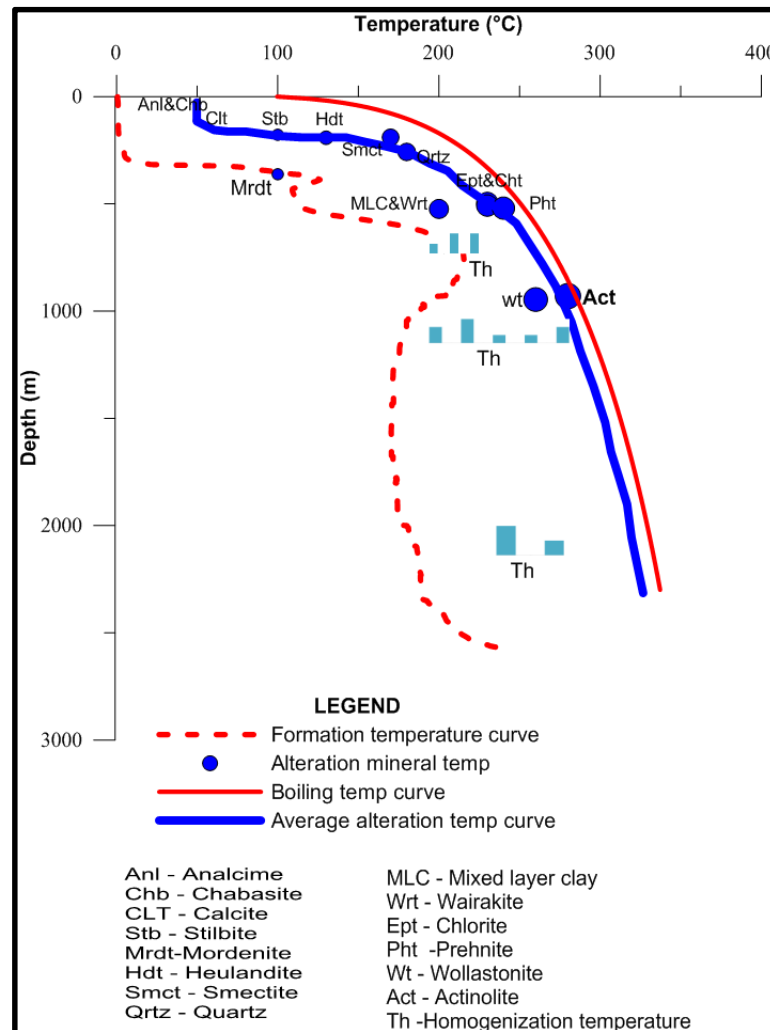


FIGURE 16: Formation, alteration mineral and boiling temperature curves compared to fluid inclusion temperatures

7. STRATIGRAPHIC CORRELATION OF WELL HE-55 TO WELLS HE-36 AND HE-57

Wells HE-55 and HE-36 are found at different locations within the Hverahlíd geothermal field and HE-57 belongs to the Gráuhnúkar field to the west (Figure 7). As described before, HE-55 was drilled towards more/less NE-SW striking faults and fissures (Figures 5 and 7).

The top of HE-55 was drilled through the lava Hellisheidarhraun D which is postglacial, about 2000 years old, while the top part of HE-36 was drilled through Hellisheidarhraun A, having an age of 10,300 years. HE-57, however, was drilled through Hellisheidarhraun B/C which has been dated at 5,500 years (Saemundsson, 1995). Geologically, the lithology of HE-55 does not contain Hellisheidarhraun A or Hellisheidarhraun B/C with reference to the top lithology (Figure 17).

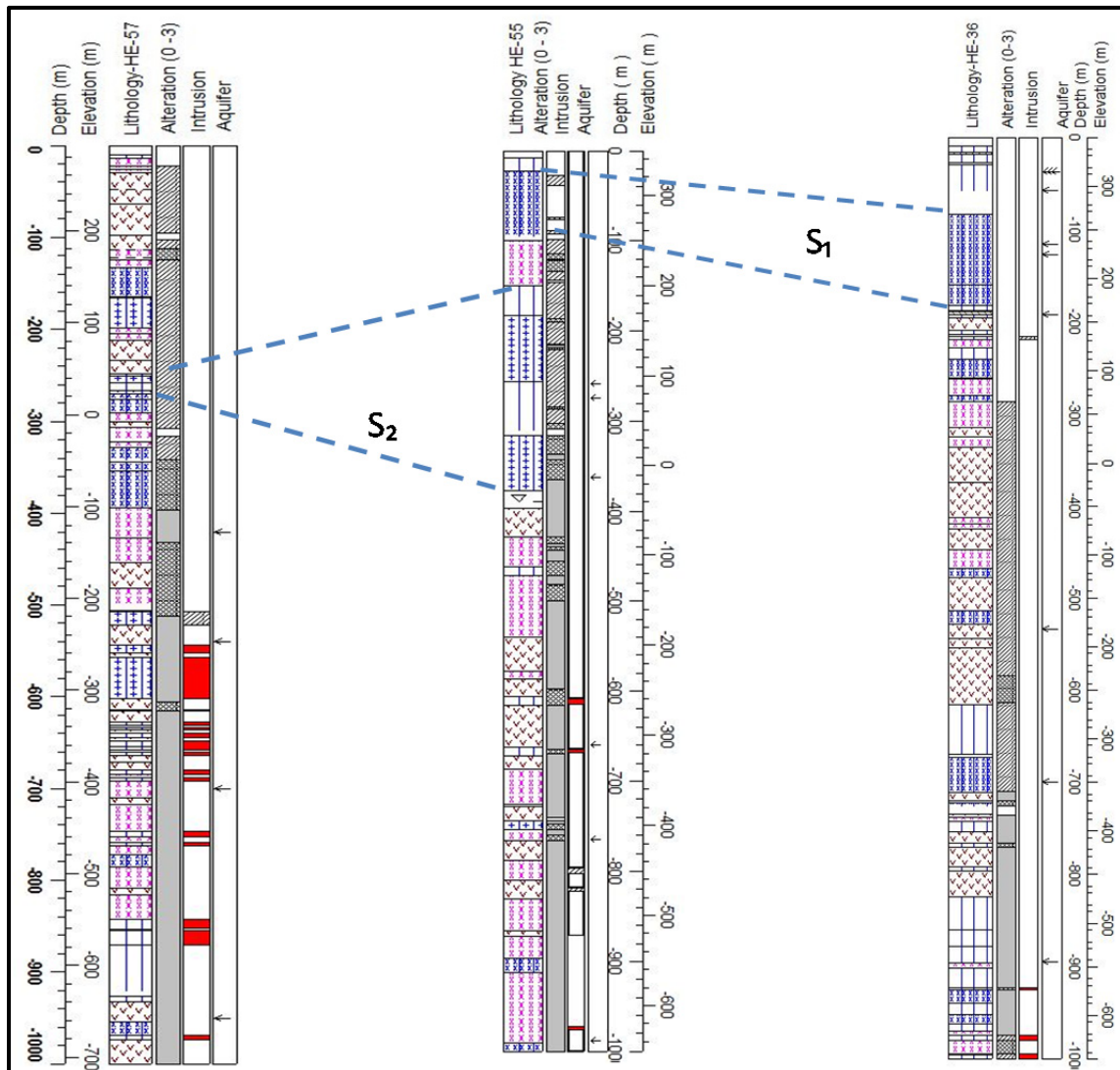


FIGURE 17: Correlation between HE-55, HE-57 and HE-36 (data for HE-36 and HE-57 extracted from Níelsson and Haraldsdóttir, 2008, and Helgadóttir, 2010, respectively)

In well HE-55, four lava flows, fine- to medium-grained, were found from 150 to 309 m depth; HE-57 also has lava flows at 250-270 m (Figure 17). In HE-55, the lava sequence extends over about 200 m, while in HE-57 it is about 20 m shown by the dotted line S_2 in Figure 17. However, the pattern of the lava flows is identical (fine- to medium-grained, medium- to coarse-grained, fine- to medium-grained); the composition is similar as are the petrographic characteristics. It was concluded that these are the same flows thinning out towards the west. In addition, the pillow basalt in HE-36 and HE-55, shown by S_1 in Figure 17, seems to be a similarly described formation in both wells in the petrographic analysis. Otherwise, no correlations were observed. This may not seem surprising as a fault/fissure zone separates HE-36 from HE-55 and another one separates HE-55 from HE-57, but the top lithology of all three wells was less affected by faults and fissures than at depth.

8. DISCUSSION

In borehole geology, the main objective is to uncover the geothermal characteristics, for example, to decide whether the system is cooling or heating up by looking at different parameters. The study of alteration minerals in HE-55 showed that calcite is dominant and forms at later stages, especially at the

bottom part of 1000 m according to time mineral-deposition sequences, which indicate that the system is cooling with time. Considering wollastonite as a calcium-silicate mineral, it appeared at 946 m depth in HE-55 which implies temperatures of about 270°C; but sometimes this mineral can form at lower temperatures, provided the CO₂ pressure is reduced (Fernandez-Caliani et al., 1998). CO₂ pressure can escape through fissures which can lead to the formation of wollastonite at lower temperatures. This may apply to well HE-55 which was drilled toward the fault zone where CO₂ pressure may be reduced and, therefore, wollastonite may have formed when the system was cooling.

However, most of the hydrothermal alteration minerals showed that low-temperature minerals started to form and were later replaced by high-temperature minerals; some low-temperature minerals did appear with high-temperature minerals, for example, smectite in the chlorite-epidote zone.

In addition, geological and hydrothermal alteration studies showed that the intensity of rock alteration and alteration minerals increased with depth (Figures 12 and 18).

Fluid inclusion analyses at the depth of 746-760 m indicated the possibility that the inclusion temperatures were in equilibrium with the formation temperature range. However, the system is cooling at greater depths of 1090-1104 m, as observed from primary fluid inclusion homogenization temperatures. These temperatures were higher than the formation temperatures, implying that during the formation of the crystals the geothermal system was hotter.

Furthermore, alteration temperatures were higher than the measured formation temperatures (Figures 16 and 18) in well HE-55, which indicates cooling of the system; this fact is supplemented by the homogenization temperatures of fluid inclusions, most of which were relatively higher than the formation temperatures. From Figure 18 it can be seen that formation temperatures show four episodes marked:

E₁–E₄: E₁– heating; E₂– cooling; E₃– heating; and E₄– cooling.

But, generally, alteration temperatures were higher than formation temperatures, which signifies cooling of the system.

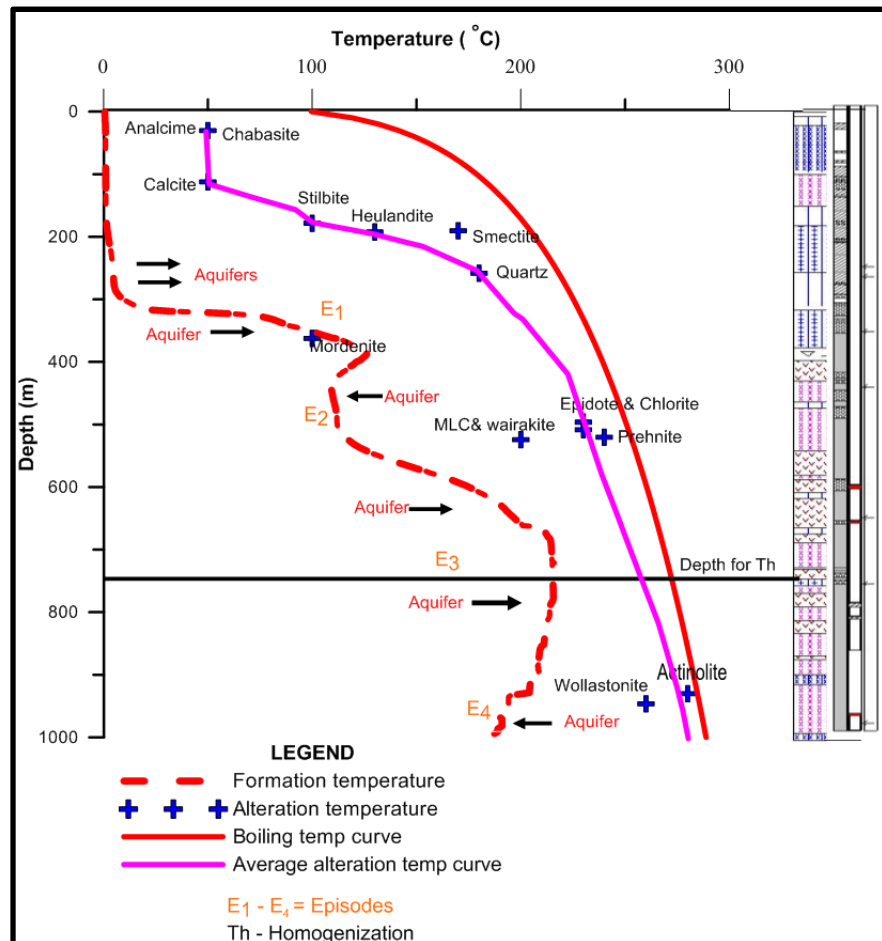


FIGURE 18: Formation temperature, alteration temperature, boiling point curve and lithology for well HE-55

9. CONCLUSIONS

From the study of the uppermost 1000 m of well HE-55 and lithological correlations with HE-57 and HE-36, the following conclusions can be drawn:

1. The lithology of well HE-55 in its upper 1000 m is mostly composed of hyaloclastite formations (basaltic tuff, basaltic breccia and pillow basalt), fine- to medium-grained and medium- to coarse-grained basalt lava flows (interglacial) intruded by some dykes of basaltic composition.
2. Four alteration zones were identified and arranged according to increases in temperature of hydrothermal alteration minerals: unaltered zone (0-114 m) with $< 50^{\circ}\text{C}$; smectite-zeolite zone at 114-496 m and $50-200^{\circ}\text{C}$; chlorite-epidote zone from 496 to 930 m with $250-275^{\circ}\text{C}$; and from 930-1000 m an epidote-actinolite zone with temperatures of $275-350^{\circ}\text{C}$.
3. Calcite is the dominant alteration mineral in the upper 1000 m and seems to be deposited later in the sequence during the cooling of the system.
4. The lithologies of HE-55, HE-57 and HE-36 do not compare except, possibly, in the upper parts of HE-55 and HE-57 where a lava sequence with identical patterns is observed with the lavas thinning out from HE-55 towards HE-57. In the upper parts of HE-55 and HE-36, the pillow basalt seems to be similar, as their descriptions are similar in petrographic analysis.
5. In the uppermost 1000 m of well HE-55, most of the alteration mineral temperatures are higher than formation temperatures; this signifies that the geothermal system is cooling.
6. Seven feed zones were located at different depth, most of these are associated with lithological boundaries and margins of intrusions.

ACKNOWLEDGEMENTS

It is my pleasure to convey my gratitude to the United Nation University Geothermal Training Programme (UNU-GTP) Director, Dr. Ingvar B. Fridleifsson, and his deputy, Mr. Lúdvík S. Georgsson, for the opportunity to participate in the 6 months geothermal training programme in Iceland. The practical approach embraced by the programme has sharpened my understanding of geothermal resources and their application. I would also like to thank the rest of the UNU-GTP staff, Mr. Ingimar G. Haraldsson, Ms. Thórhildur Ísberg, Ms. Dorthe H. Holm and Mr. Markús A.G. Wilde, for their support before and during the training.

Many thanks go to my supervisors, Dr. Björn S. Hardarson, and Dr. Hjalti Franzson, for their generous support, guidance and for sharing their experience during my entire project period. I acknowledge the timely technical support and contributions from Dr. Gudmundur Ómar Fridleifsson, Ms. Anette K. Mortensen, Mr. Sigurdur Sveinn, Ms. Sandra Ósk, and Ms. Christa Feucht, Sigurveig, Signý and all resource persons from ISOR offered during lectures, fieldwork and laboratory analysis. This research could not have been completed without generous data from Reykjavik Energy, to whom I am grateful.

Special thanks go to the Commissioner for Energy and Petroleum Affairs, and the Ministry of Energy and Minerals for allowing me to participate in the geothermal training programme. I also appreciate the encouragement given by my colleagues from the Ministry of Energy and Minerals.

The studies would not have been easy without the cooperation of my fellow geologists, Mr. Convine Omondi Nyamweya, Mr. Isa Lugaizi, and all the UNU-GTP Fellows 2011; I am grateful.

Finally, I would like to thank my family for their support and encouragement. God bless you all.

REFERENCES

- Ahmed Youssouf, M., 2008: Borehole geology and hydrothermal mineralization of well HN-08, Hellisheidi geothermal field, SW-Iceland. Report 8 in: *Geothermal training in Iceland 2008*. UNU-GTP, Iceland, 1-29.
- Alnethary, M.F.A., 2010: Borehole geology and alteration mineralogy of well HE-52, Hellisheidi in SW-Iceland. Report 9 in: *Geothermal training in Iceland 2010*. UNU-GTP, Iceland, 71-98.
- Árnason, K., 2007: *TEM – resistivity measurements in the Hengill area in 2006 and proposal for exploration drilling at Eldborg*. ÍSOR – Iceland GeoSurvey, Reykjavík, report ÍSOR2007/005 (in Icelandic), 34 pp.
- Björnsson, G., 2004: Reservoir conditions at 3-6 km depth in the Hellisheidi geothermal field, SW-Iceland, estimated by deep drilling, cold water injection and seismic monitoring. *Proceedings of the 29th Workshop on Geothermal Reservoir Engineering, Stanford University, Stanford, CA*, 26-28.
- Browne, P.R.L., 1978: Hydrothermal alteration in active geothermal fields. *Annual Reviews of Earth and Planetary Science*, 6, 229-250.
- Dauteuil, O., Bouffette, J., Tournat, F., Van, Vliet-Lanoë, B., Embry, J.C., and Quété, Y., 2005: Holocene vertical deformation outside the active rift zone of northern Iceland. *Tectonophysics*, 404-3/4, 203-216.
- Fernandez-Caliani, J.C., and Galan, E., 1998: Effect of fluid infiltration on wollastonite genesis at the Merida contact – metamorphic deposits, SW-Spain. *Mineralogy and Petrology*, 62, 247-267.
- Foulger, G.R., and Toomey, D.R., 1989: Structure and evolution of the Hengill-Grensdalur volcanic complex, Iceland: Geology, geophysics and seismic tomography. *J. Geophys. Res.*, 94-B12, 17,511-17,522.
- Franzson, H., 1998: Reservoir geology of the Nesjavellir high-temperature field in SW-Iceland. *Proceedings of the 19th Annual PNOC-EDC Geothermal Conference, Manila*, 13-20.
- Franzson, H., 2011: *Borehole geology*. UNU-GTP, Iceland, unpublished lecture notes.
- Franzson, H., Gunnlaugsson, E., Árnason, K., Saemundsson, K., Steingrímsson, B., and Hardarson, B., 2010: The Hengill geothermal system, conceptual model and thermal evolution. *Proceedings of the World Geothermal Congress 2010, Bali, Indonesia*, 9 pp.
- Franzson, H., Kristjánsson, B.R., Gunnarsson, G., Björnsson, G., Hjartarson, A., Steingrímsson, B., Gunnlaugsson, E., and Gíslason, G., 2005: The Hengill Hellisheidi geothermal field. Development of a conceptual geothermal model. *Proceedings of the World Geothermal Congress 2005, Antalya, Turkey*, 7 pp.
- Gebrehiwot M., K., 2010: *Subsurface geology, hydrothermal alteration and geothermal model of Northern Skardsmýrarfjall, Hellisheidi geothermal field, SW Iceland*. University of Iceland, MSc thesis, UNU-GTP, Iceland, report 5, 65 pp.
- Gudfinnsson, G.H., Helgadóttir, H.M., and Tryggvason, H., 2010a: *Hverahlíd – borehole HE-55, Pre-drilling, 1st and 2nd stages: Drilling for surface casing to 102 m, anchor casing to 309 m and production casing to 810 m depth*. ÍSOR – Iceland GeoSurvey, Reykjavík, report ÍSOR-2010/058 (in Icelandic), 49 pp.

Gudfinnsson, G.H., Helgadóttir, H.M., and Tryggvason, H., 2010b: *Hverahlid – borehole HE-55, 3rd stage: Drilling for production part from 810 m depth to 2782 m.* ÍSOR – Iceland GeoSurvey, Reykjavík, report ÍSOR-2010/096 (in Icelandic), 73 pp.

Gudmundsson, Á., 1992: Formation and growth of normal faults at the divergent plate boundary in Iceland. *Terra Nova*, 4-4, 464-471.

Gudmundsson, Á., 1998: Magma chambers modelled as cavities explain the formation of rift zone central volcanoes and their eruption and intrusion statistics. *J. Geophys. Res.*, 103-B4, 7401-7412.

Hardarson, B.S., Fitton, J.G., and Pringle, M.S., 1997: Rift relocation - a geochemical and geochronological investigation of a paleo-rift in Northwest Iceland. *Earth Planet Sci. Lett.*, 153, 181-196.

Hardarson, B.S., Einarsson, G.M., Kristjánsson, B.R., Gunnarsson, G., Helgadóttir, H.M., Franzson, H., Árnason, K., Ágústsson, K., and Gunnlaugsson, E., 2010: Geothermal reinjection at the Hengill triple-junction, SW Iceland. *Proceedings of the World Geothermal Congress 2010, Bali, Indonesia*, 7 pp.

Helgadóttir, H.M., 2010: *Gráuhnúkar – borehole HE-57, Pre-drilling, 1st and 2nd stages: Drilling for surface casing to 95 m, anchor casing to 343 m and production casing to 1040 m depth.* ÍSOR – Iceland GeoSurvey, Reykjavík, report ÍSOR-2010/004 (in Icelandic), 101 pp.

Helgadóttir, H., Snaebjörnsdóttir, S., Nielsson, S., Gunnarsdóttir, S., Matthíasdóttir, T., Hardarson, B., Einarsson, G., and Franzson, H., 2010: Geology and hydrothermal alteration in the reservoir of the Hellisheidi high temperature system, SW-Iceland. *Proceedings of the World Geothermal Congress 2010, Bali, Indonesia*, 10 pp.

Hjartarson, Á., 2009: *Central volcanoes as indicators for the spreading rate in Iceland.* ÍSOR – Iceland GeoSurvey, Reykjavík, unpubl. report.

Jakobsson, S.P., Jónasson, K., and Sigurdsson, I.A., 2008: The three igneous rock series of Iceland. *Jökull*, 58, 117-138.

Jóhannesson H., and Saemundsson, K., 1999. *Geological map 1:1.000.000.* Icelandic Institute of Natural History.

Koestono, H., 2007: Borehole geology and hydrothermal alteration of well HE-24, Hellisheidi geothermal field, SW-Iceland. Report 10 in: *Geothermal Training in Iceland, 2007.* UNU-GTP, Iceland 199-224.

Kristmannsdóttir, H., 1975: Hydrothermal alteration of basaltic rocks in Icelandic geothermal areas. *Proceedings of the 2nd U.N. Symposium on the Development and Use of Geothermal Resources, San Francisco*, 441-445.

Kristmannsdóttir, H., 1977: Types of clay minerals in altered basaltic rocks, Reykjanes, Iceland. *Jökull*, 26 (in Icelandic with English summary), 3-39.

Kristmannsdóttir, H., 1979: Alteration of basaltic rocks by hydrothermal activity at 100-300°C. In: Mortland, M.M., and Farmer, V.C. (editors), *International Clay Conference 1978.* Elsevier Scientific Publishing Co., Amsterdam, 359-367.

Mbia, P.K., 2010: Borehole geology and hydrothermal alterations of well HE-39, Hellisheidi in SW-Iceland. Report 19 in: *Geothermal training in Iceland 2010.* UNU-GTP, Iceland, 337-360.

- Mostaghel, B., 1999: Processing and interpretation of geophysical well logs from well KJ-32, Krafla geothermal field, NE-Iceland. Report 8 in: *Geothermal training in Iceland 1999*. UNU-GTP, Iceland 193-220.
- Níelsson, S., and Franzson, H., 2010: Geology and hydrothermal alteration of the Hverahlíd HT system, SW-Iceland. *Proceedings of the World Geothermal Congress 2010, Bali, Indonesia*, 6 pp.
- Níelsson, S., and Haraldsdóttir, S.H., 2008: *Hverahlíd – borehole HE-36, Pre-drilling, 1st and 2nd stages: Drilling for surface casing to 105 m, anchor casing to 364 m and production casing to 1104 m depth*. ÍSOR – Iceland GeoSurvey, Reykjavík, report ÍSOR-2008/012 (in Icelandic), 102 pp.
- Njue, L.M., 2010: Borehole geology and hydrothermal mineralization of well HE-27, Hellisheidi in SW-Iceland. Report 24 in: *Geothermal training in Iceland 2010*. UNU-GTP, Iceland, 463-492.
- Pálmason, G., and Saemundsson K., 1974: Iceland in relation to the Mid-Atlantic Ridge. *Annual Review Earth Planet. Sci.*, 2, 25-50.
- Pendon, R.R., 2006: Borehole geology and hydrothermal mineralisation of well HE-22, Ölkelduháls field, Hengill area, SW-Iceland. Report 17 in: *Geothermal training in Iceland 2006*. UNU-GTP, Iceland, 357-390.
- Reyes, A.G., 1990: Petrology of Philippine geothermal systems and the application of alteration mineralogy to their assessment. *J. Volc. Geoth. Res.*, 43, 279-309.
- Reyes, A.G., 2000: *Petrology and mineral alteration in hydrothermal systems: from diagenesis to volcanic catastrophes*. UNU-GTP, Iceland, report 18-1998, 77 pp.
- RockWare Inc., 2007: *LogPlot program*. Rockware Inc.
- Saemundsson, K., 1979: Outline of the geology of Iceland. *Jökull*, 29, 7-28.
- Saemundsson, K., 1995: *Geothermal and hydrothermal map of the Hengill area, 1:25,000*. Orkustofnun, Reykjavík.
- Saemundsson, K., and Gunnlaugsson, E., 2002: *Icelandic rocks and minerals*. Edda and Media Publishing, Reykjavík, Iceland, 233 pp.
- Senior, A.L., Cinotto, J.P., Conger, W.R., Bird, H.P., and Pracht, A.K., 2005: *Interpretation of geophysical logs, aquifer tests, and water levels in wells in and near the North Penn Area 7 Superfund site, Upper Gwynedd Township, Montgomery County, Pennsylvania*. US Geological Survey, scientific investigations report, 2005-5069, 2000-02.
- Sigmundsson, F., and Saemundsson, K., 2008: Iceland: A window on North-Atlantic divergent plate tectonics and geologic processes. *Episodes*, 31-1, 92-97.
- Simmons, S.F., and Christenson, B.W., 1994: Origin of calcite in a boiling geothermal system. *Am. Jour. Sci.*, 294, 361-400.
- Thompson, A.J.B., and Thompson, J.F.H., (editors), 1996: *Atlas of alteration: A field and petrographic guide to hydrothermal alteration minerals*. Alpine Press Ltd., Vancouver, British Columbia, 119 pp.
- Thórdarson, T., and Höskuldsson, Á., 2008: Postglacial volcanism in Iceland. *Jökull*, 58, 197-228.
- Wolfe, C.J., Bjarnason, I.T., Van Decar, J.C, and Solomon, S.C., 1997: Seismic structure of the Iceland plume. *Nature*, 385, 245-247.

APPENDIX I: XRD clay analysis results

Sample number	Depth (m)	Untreated sample (Å)	Glycolated sample (Å)	Heated sample (Å)	Mineral
1	170	13.66	13.7	10	Smectite
2	284	13.7	13.895	10	Smectite
3	354	13.52	13.62	10	Smectite
4	434	14.85	15.12	10	Smectite
5	495	17.47/14.87/7.74	17.67/7.24/14.9	14/10	MLC, chlorite and smectite
6	510	14.79	14.8	14	MLC & Chlorite
7	520	32.33/13.88	32.38/14.77	10	Mixed-layer clay
8	540	30.337/14.29	30.36/13.97	10.523	Smectite & Chlorite
9	560	32.85/15.78	33.080	12	Mixed-layer clay
10	580	31.67/14.56	32/14.662	12	MLC & Chlorite
11	600	31.12/14.3	30.04/14.4	12	MLC & Chlorite
12	620	30/14	30.1/14.1	12	MLC & Chlorite
13	680	-	-	-	No clay
14	730	14/17	14/17.59	10/12	MLC & Smectite
15	780	14.4	14.5	-	Smectite & Chlorite
16	880	18.75/17.68/14	18.8/17.7/14	11	MLC & Chlorite
17	980	17.3	17.56	14	MLC & Chlorite

APPENDIX II: Characteristic XRD patterns for the clay minerals of well HE-55

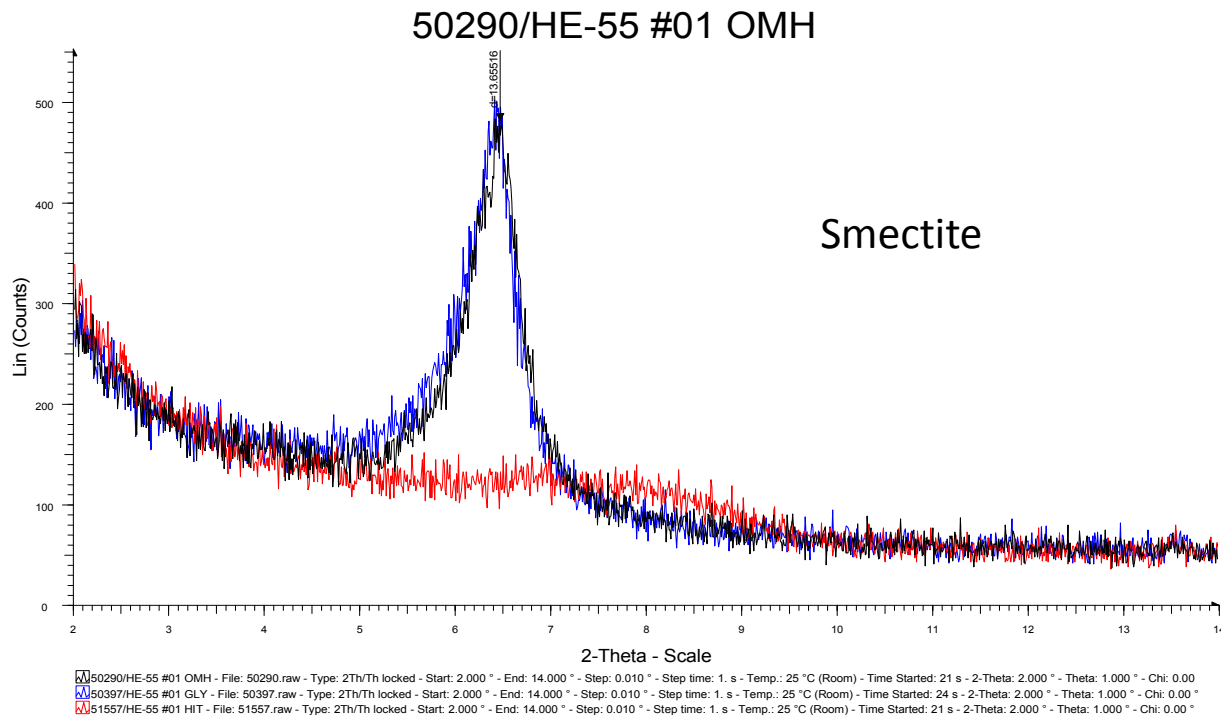


FIGURE 1: Smectite

50294/HE-55 #05 OMH

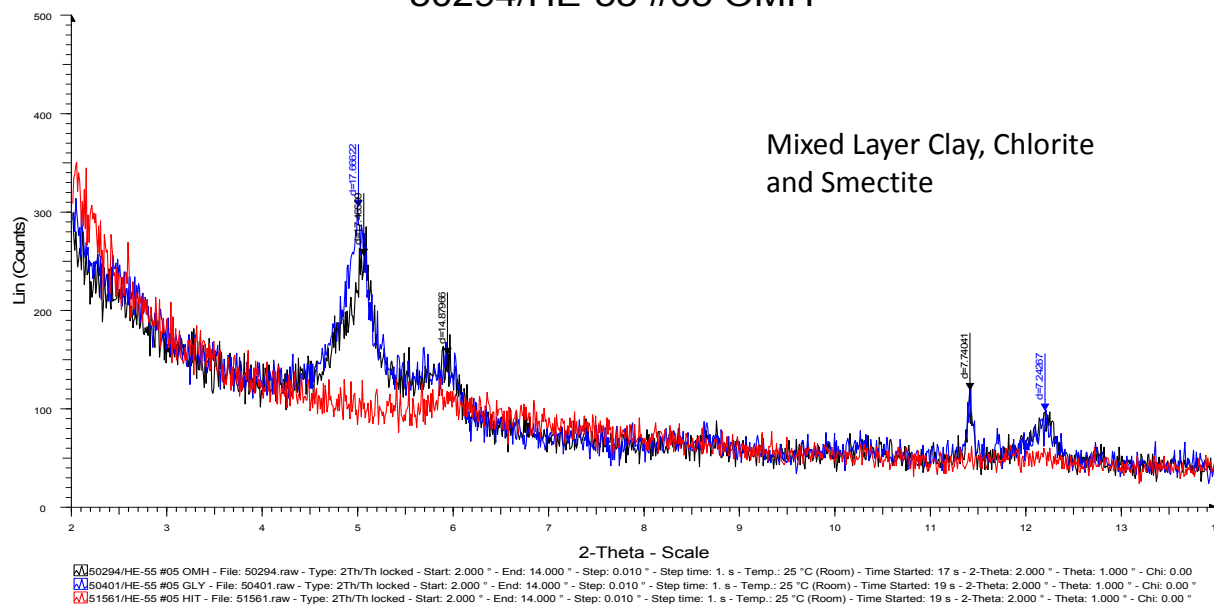


FIGURE 2: Mixed-layer clay, smectite and chlorite

50298/HE-55 #09 OMH

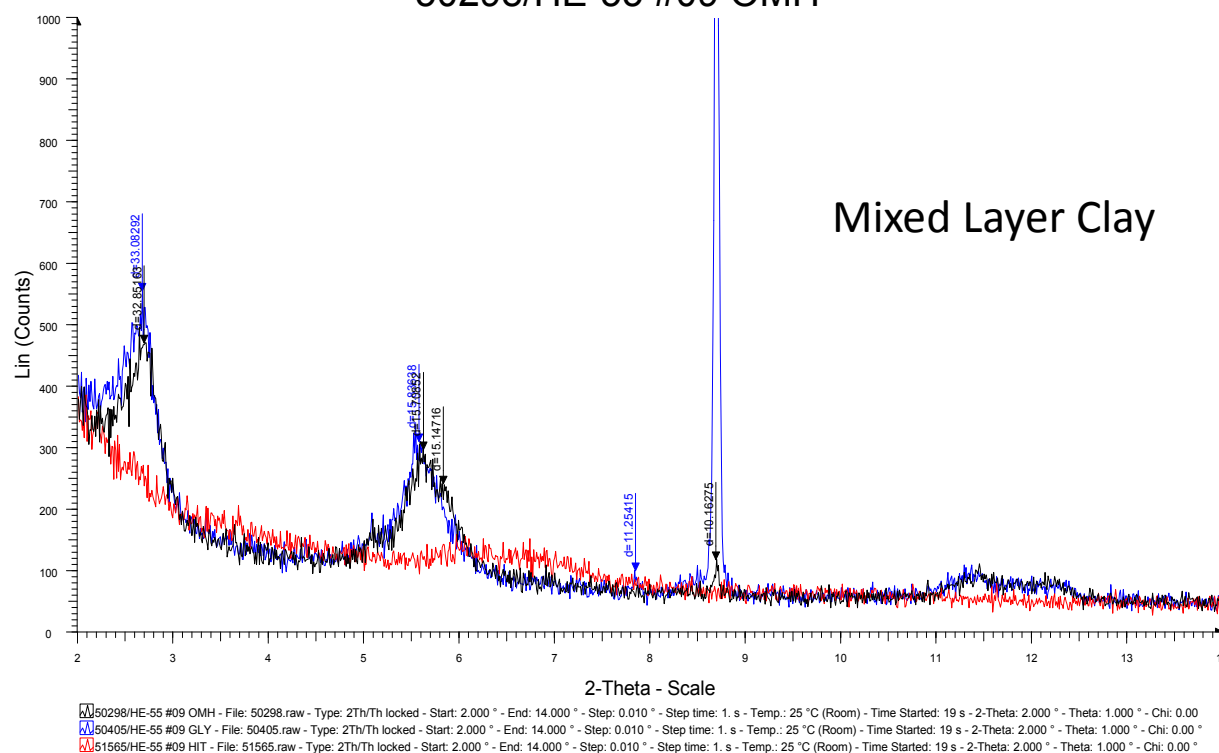


FIGURE 3: Mixed-layer clay

50302/HE-55 #13 OMH

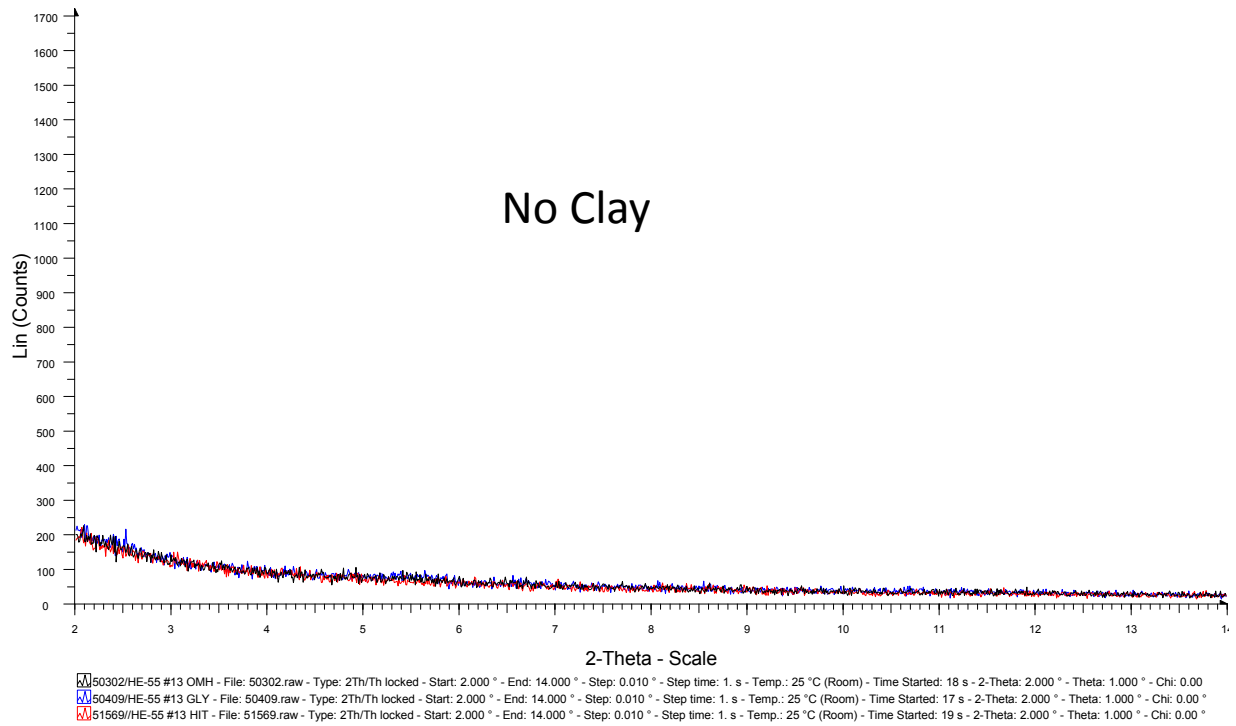


FIGURE 4: No clay